

Software Benchmarking of the 2nd round CAESAR Candidates

Ralph Ankele¹ and Robin Ankele²

¹ Information Security Group, Royal Holloway, University of London
McCrea Building, Egham TW20 0EX, UK

ralph.ankele.2015@rhul.ac.uk

² Department of Computer Science, University of Oxford
Wolfson Building, Oxford OX1 3QD, UK

robin.ankele@cs.ox.ac.uk

Abstract. The software performance of cryptographic schemes is an important factor in the decision to include such a scheme in real-world protocols like TLS, SSH or IPsec. In this paper, we develop a benchmarking framework to perform software performance measurements on authenticated encryption schemes. In particular, we apply our framework to independently benchmark the 29 remaining 2nd round candidates of the CAESAR competition. Many of these candidates have multiple parameter choices, or deploy software optimised versions raising our total number of benchmarked implementations to 232. We illustrate our results in various diagrams and hope that our contribution helps developers to find an appropriate cipher in their selection choice.

Keywords: Software benchmarks · CAESAR · 2nd round candidates · real-worlds usecases · tls · ssh · optimisations · aes-ni · sse · avx · neon

1 Introduction

An authenticated encryption (AE) scheme provides confidentiality, integrity and authenticity simultaneously. These goals are typically achieved by combining separate cryptographic primitives, an encryption scheme to ensure confidentiality and a message authentication code for integrity and authenticity. However, the generic composition, the combination of a confidentiality mode with an authentication mode, may lead to implementation errors and is often not efficient (*e.g.* the input stream has to be processed twice, for the encryption scheme and the message authentication code). Recently, some practical attacks [CHVV03], [Vau02] have confirmed the vulnerability of these AE schemes. In 2013, the CAESAR [Ber14] competition was announced in order to mitigate such attacks. Moreover, the aim of the newly proposed candidates was to achieve fast and efficient execution and to be suitable for widespread adoption. In March 2014, 57 first round candidates were submitted to the CAESAR competition. Abed *et al.* [AFL14] provide a classification and a general overview of the first round candidates. In July 2015, the second round candidates were announced. The deadline for the announcement of the third round candidates is expected in end July 2016 that requires the CAESAR committee to make a selection decision which candidates will be included in the third round.

Beside of the security guarantees of the authenticated encryption mode, the software and hardware performance of the candidate becomes more and more important. One of the requirements imposed on all CAESAR submissions was that they should demonstrate the potential to be superior to AES-GCM in at least one significant aspect. One of those aspects that is particularly significant for the usage in widely deployed protocols

such as TLS, SSH and IPsec is software performance. Therefore, we have developed a benchmarking framework for automated and accurate software performance measurements and applied it to benchmark the remaining 29 second round candidates. Many of these candidates have multiple parameter choices, extending the number to 125 implementations. Overall, we have considered several software performance optimised implementations, raising the total number of benchmarked implementations to 232.

During our benchmarks, we perform and illustrate our measurements on a continuous function (with message and associated data sizes from 0 to 2048 bytes, in 128 byte steps) and on some fixed length sizes, relating to real-world usecases — 1 byte (one keystroke, SSH), 16 bytes (small payload), 557 bytes (average IP packet size), 1.5 kB (ethernet MTU size, TLS), 16 kB (max. TCP packet size) and 1 MB (*e.g.* file upload).

Related Work. In order to evaluate the software performance of the CAESAR candidates, Bernstein provides the SUPERCOP* [Ber16] framework, which is a general purpose framework for the evaluation of the software performance of cryptographic software. Saarinen presented the BRUTUS† [Saa16] framework, in order to test the CAESAR candidates for cryptographic weaknesses. Additionally to the software performance of the candidates, the hardware performance is also an important factor in the selection of the final portfolio. Homsirikamol *et al.* [HDF⁺15] present a hardware API to perform hardware benchmarks of the CAESAR candidates.

Contribution and Outline. In this paper, we present a complementary benchmarking framework to perform automatic and accurate measurements on authenticated encryption functions. We apply this framework to perform independent software benchmarks on the 2nd round CAESAR candidates and illustrate the results in various diagrams.

This paper is organised as follows. In Section 2, we introduce the 2nd round candidates of the CAESAR competition and classify them regarding their underlying cryptographic primitive. Section 3, presents our benchmarking framework and the measurement settings. In Section 4, we give an overview and discuss the software optimisation implemented in the 2nd round candidates. Finally, in Section 5 we present the results of the benchmarking and Section 6 concludes the paper.

2 Classification of the 2nd round CAESAR Candidates

In the CAESAR [Ber14] call for submissions the choice of underlying primitive and type of cipher was open for the designers. After 57 submissions for the first round, 29 submissions have been selected for the second round. Within these remaining candidates there are 15 based on block ciphers, 8 based on sponge constructions, 4 based on stream ciphers, 2 based on permutations and 1 based on a compression function. Table 1 gives an overview of the 2nd round candidates of the CAESAR competition sorted by type.

Some of the candidates are *online*. An online cipher is defined such that the encryption of message block M_i is only depending on already processed message blocks M_1, \dots, M_{i-1} . Furthermore, an inverse-free scheme indicates if the inverse of an underlying primitive is needed (*i.e.* for the purpose of decryption of the underlying block cipher). An authenticated encryption scheme is nonce-misuse resistant, if the cipher is still secure under the repetition of nonces. Moreover, we can distinguish between nonce misuse resistance for online and offline ciphers. On the one hand, offline ciphers security can be claimed if the repetition of the ciphers leak only the ability to see a repeated message. On the other hand, for online ciphers security can be claimed, if nonces are repeated only the common prefix of the messages can be observed.

*<https://bench.cr.yp.to/supercop.html>

†<https://github.com/mjosaarinen/brutus>

Table 1: Overview of the 2nd round CAESAR candidates.[‡] Possible types of schemes are: BC: block cipher based schemes, SC: stream cipher based schemes, Sponge: scheme based on Sponge construction (duplex or otherwise), P: permutation based scheme and CF: scheme based on compression function. Underlying primitives are: AES: when the full AES-128 is used, AES[r]: when a round reduced version of AES is used, other dedicated primitive or constructions: e.g. SHA2, SPN, LFSR. Entries for nonce misuse resistance are: None: when no security is claimed by the designers if nonces are repeated, Max: when for offline ciphers the repetition of nonces only leak the ability to see a repeated message, LCP: for online ciphers, all an adversary can observe is the longest common prefix of messages for repeated nonces

Name	Type	Primitive	Parallel Enc. / Dec.	Online Enc. / Dec.	Inverse- free	Security proof	Nonce mis- use resistant	Reference	Software Version
AEGIS	BC	AES[1]	✓ / -	✓ / ✓	-	-	None	[WP14]	v1*
AES-COPA	BC	AES	partly/partly	✓ / ✓	-	✓	LCP	[ABL+15]	v2**
AES-JAMBU	BC	AES, Simon	- / -	✓ / ✓	✓	-	LCP	[WH15]	v2*
AES-OTR	BC	AES	✓ / ✓	✓ / ✓	✓	✓	None	[Min16]	v3*
AEZ	BC	AES[4]	✓ / ✓	- / -	✓	✓	Max	[HKR15]	v4*
CLOC	BC	AES, TWINE	- / -	✓ / ✓	-	✓	None	[IMG15]	v2 [◇]
Deoxys	BC	AES	✓ / ✓	✓ / ✓	-	✓	LCP	[JNP15a]	v1.3*
ELmD	BC	AES	partly/partly	✓ / ✓	-	✓	LCP	[DN15]	v2*
Joltik	BC	Joltik-BC	✓ / ✓	✓ / ✓	-	✓	LCP	[JNP15b]	v1.3*
OCB	BC	AES	✓ / ✓	✓ / ✓	-	✓	None	[KR14]	v1*
POET	BC	AES	partly/partly	✓ / ✓	✓	✓	LCP	[AFF+15]	v2**
SCREAM	BC	SPN	✓ / ✓	✓ / ✓	-	-	None	[GLS+15]	v3*
SHELL	BC	AES	partly/partly	✓ / ✓	-	✓	None	[Wan15]	v2*
SILC	BC	AES, Present, LED	- / -	✓ / ✓	✓	✓	None	[IMG+15]	v2 [◇]
Tiaoxin	BC	AES[1]	✓ / ✓	✓ / ✓	✓	-	None	[Nik15]	v2*
OMD	CF	SHA2	- / -	✓ / ✓	-	✓	None	[CMN+15]	v2*
Minalpher	P	SPN	✓ / ✓	✓ / ✓	-	✓		[STA+15]	v1.1 [♠]
PAEQ	P	AESQ	✓ / ✓	✓ / ✓	✓	✓		[BK14]	v1**
ACORN	SC	LFSR	✓ / ✓	✓ / ✓	✓	-	None	[Wu15]	v2*
HS1-SIV	SC	ChaCha/Poly1305	- / -	- / -	✓	✓	Max	[Kro15]	v1*
MORUS	SC	LRX	- / -	✓ / ✓	✓	-	None	[HW15]	v1*
TriviumA-ck	SC	Trivium	partly/partly	- / -	✓	✓	None	[CM15]	v2*
Ascon	Sponge	SPN	- / -	✓ / ✓	✓	✓		[DEMS15]	v1.1**
ICEPOLE	Sponge	Keccak-like	✓ / ✓	✓ / ✓	✓	✓		[MGH+15]	v2*
Ketje	Sponge	Keccak-f	- / -	✓ / ✓	✓	✓	None	[BDP+14]	v1 [♣]
Keyak	Sponge	Keccak-f	✓ / ✓	✓ / ✓	✓	✓	None	[BDP+15]	v2 [♣]
NORX	Sponge	LRX	✓ / ✓	✓ / ✓	✓	✓	None	[AJN15]	v1 [♡]
π -cipher	Sponge	ARX	✓ / ✓	✓ / ✓	✓	✓	Intermediate	[GMS+15]	v2 [□]
PRIMATEs	Sponge	SPN	- / -	✓ / ✓	✓	✓	LCP	[ABB+14]	v1**
STRIBOB	Sponge	Streebog	- / -	✓ / ✓	✓	✓	None	[OSB15]	v2**

[‡] Data obtained from: <https://aezoo.compute.dtu.dk/doku.php>

* Source code obtained via email from designer.

** Source code from SUPERCOP v20140622 obtained from <https://bench.cr.yp.to/supercop.html>.

♡ Source code received from <https://github.com/norx/norx>.

◇ Source code received from <http://www.nuee.nagoya-u.ac.jp/labs/tiwata/AE>.

♣ Source code received from <https://github.com/gvanas/KeccakCodePackage>.

♠ Source code received from <http://info.isl.ntt.co.jp/crypt/minalpher/web/downloads.html>.

□ Source code received from <http://pi-cipher.org>.

3 Benchmarking Framework

Similar to the SUPERCOP [Ber16] and BRUTUS [Saa16] frameworks, we have developed a benchmarking framework to facilitate automatic software performance evaluations for authenticated encryption functions. Using our toolkit, one can perform independent and accurate software performance measurements (*i.e.* timing measurements), review the implementation of the cipher under test, generate and illustrate statistical information

Table 2: Comparison between prior benchmarking frameworks for authenticated encryption schemes and our approach.

Name	Timing Method	Noise Reduction	Accuracy	Simplicity	Applicability	Visualisation	Use Cases
SUPERCOP	RDTS+CPUID	none*	high	complex	wide range‡	none♡	0 - 2KB (1bit) and add. settings♣
BRUTUS	clock()	none	average	simple	AE ciphers	none	16, 64, 256, 1k, 4k, 16k, and 65kB
This paper	RDTS	averaging and median†	high	complex§	AE ciphers	2d, 3d and bar plots	0 - 2KB (128bit) and see Table 3

* Release of multiple measurements of the same function for post processing (median and quartiles) on web page. Recommendation to turn off hyper-threading and over-clocking as well as recommendation to perform measurement when the computer is in an idle state.

† Measurements performed in single user mode.

§ An updated version of our framework aims to provide automated benchmarking and more user-friendliness.

‡ Hash functions, stream ciphers, signature schemes, secret sharing, encryption and AE schemes

♡ Unclear and crowded 2d plots available at <https://bench.cr.yp.to/results-aead.html>

♣ Additionally settings include (all in the same ranges): forgery of message, only message, and only ad processing.

about the software performance, and compare different parameters and optimisations of a cipher among its different optimisations or to other ciphers under test. More specifically, the benchmarking functionality is implemented in C programming language and can be compiled on various platforms. Moreover, in order allow for semi-automatic testing, we supply cmake and other script based functionalities (*i.e.* bash scripts for compiling and benchmarking of the software candidates under test). In order to illustrate and visualise the results of the benchmarking and to promote reasonable comparison between the software candidates, we supply some visualisation scripts runnable in a Matlab environment. Our benchmarking suite is currently optimised to perform measurements of authenticated encryption functions. Nevertheless, it remains open to be extended to perform benchmarking of other functionality, and include other types of software tests. Generally, our benchmarking framework provides the following benefits compared to the SUPERCOP and BRUTUS framework.

- ◇ Very simple with only focus on comparison of AE schemes.
- ◇ Due to its simplicity open for extension of other software performance tests.
- ◇ Optimised TSC instruction (*i.e.* `rdts`) for accurate timing measurements.
- ◇ Reduction of noise in the measurement using single user mode, averaging and median.
- ◇ Benchmarking, review, illustration and comparison of results.

Using our framework, we built and benchmarked the 2nd round candidates (see Table 1) of the ongoing CAESAR competition. By July 2016, this includes the implementations of 29 candidates. Many of these candidates have multiple parameter choices, extending the number to 125 implementations. Overall, we have considered several software performance optimised implementations, raising the total number of benchmarked implementations to 232‡.

3.1 Measurement Setup

For our measurements we had two different measurement setups. The first measurements were taken on a 64-bit Sandy Bridge 2.3GHz dual-core Intel Core i5-2415M processor. The underlying hardware was a Mac Book Pro Early 2011 running OS X 10.11 (El Capitan) in single user mode. The second measurements were taken on a 64-bit Skylake

‡Number of implementations supported by our benchmarking hardware.

Table 3: Real-world use case settings for our benchmarking.

Message Size	Associated Data Size	Comments
1 byte	5 byte	one keystroke (<i>e.g.</i> SSH)
16 bytes	5 byte	small payload
557 byte	5 byte	average IP packet size*
1.5 kB	5 byte	ethernet MTU, TLS
16 kB	5 byte	max TCP packet size
1 MB	5 byte	file upload

* <http://slaptijack.com/networking/average-ip-packet-size>

2.4GHz dual-core Intel Core i5-6300U processor. The underlying hardware was a DELL Latitude E7470 running Ubuntu 16.04 in single user mode. The implementations under test were built using the clang compiler version 6.1.0 (clang-602.0.53) and the gcc compiler version 5.4.0 (5.4.0-6ubuntu1-16.04.2). Additionally, we enabled the following compiler flags for compile time optimisation of the underlying source code: `-Ofast -fno-stack-protector -march=native`. In order to get rid of the noise (*e.g.* context switches) during the measurement and to get a clean and stable result in an uninterrupted environment, we choose to boot in the single user mode, which just starts the core operating system and provides a `sh` command interface, without starting other core elements of the OS X operating system (*e.g.* network services, multi-user support, graphical user interface) that may interfere with our benchmarking. Furthermore, we used the same method as described in the paper from Krovetz and Rogaway [KR11]. In their approach, they determine the performance of the underlying function as the median of 91 averaged timings of 200 measurements each.

3.2 High Resolution Methods for CPU Timing Information

In general, there are several ways to determine the software performance of a function under test. Each operating system offers several methods of accurate timing sources to be used to determine the runtime (*e.g.* latency) or throughput of a function. Using multi-core processors, one must be aware of handling hyper-threading and over-clocking of the CPU during their benchmarking, to avoid distorted or falsified measurements.

For the performance of high precision timing measurements on Windows platforms, one could use the HPET (i.e. High Precision Event Timer) or the `QueryPerformanceCounter`. On Unix based platforms one can use the posix conform `time()` and `clock()` functions, as used in the BRUTUS framework. However, a much more accurate timing source on x86 processors is the Timer Stamp Counter (TSC) as used in the SUPER COP framework. The TSC is a 64 bit register and counts the number of cycles since the last reset of the machine. Using the `RDTSC` assembler instruction, one can read out the current TSC value and use it for accurate timing measurements.

In newer processor hardware, Intel processors practice out-of-order execution, where instructions are not always performed in the order as they appear in the source code. This could lead to a skewed measurement result. To avoid such errors, the `CPUID` instruction, a serialisation instruction, can be inserted, which forces every preceding instruction to complete before the execution of the `RDTSC` instruction. In our framework, we make use of the `RDTSCP` [Pao10] instruction, which is an optimised versions of the combination `CPUID` + `RDTSC`.

Table 4: Most common optimisations for the CAESAR candidates

Instruction Set	Vendor	Microarchitecture	CAESAR Candidate
AES-NI	Intel	Westmere	OCB, OTR, AEGIS, CLOC, SILC, POET, JAMBU, AEZ, Deoxys, PAEQ, Tiaoxin, TriviA-ck
SSE	Intel	Pentium III	OCB, CLOC, Keyak, Morus, OMD, Scream, Stribob, Tiaoxin, TriviA-ck
AVX	Intel	Sandy Bridge	NORX, OMD
AVX2	Intel	Haswell	Keyak, Minalpher, Morus, NORX
NEON	ARM	ARMv7-A	OCB, NORX, Scream, Stribob

3.3 Authenticated Encryption Benchmarking Settings and Real-World Usecases

In our benchmarking, we implemented measurements on a continuous function (*i.e.* where we vary the message size and the associated data size) and over some fixed message and associated data sizes (*i.e.* representing some real-world usecases).

Overall, we consider message size from 0 to 1 MB and associated data size from 0 to 2 KB. The sizes of the key and nonce are fixed-size values, as determined by the CAESAR specification. In the case of the continuous function we consider message and associated data size from 0 to 2048 bytes in 128 byte steps. On the other hand, for the timing measurements with fixed message and associated data size, we consider the values in Table 3.

The associated data is fixed to 5 bytes[§] for all measurements, which represents the typical size of the header of a TLS packet. Additionally, for better comparability, we represent the performance results of the authenticated encryption candidates in cycle per byte (cbp), which is a function of the throughput of the ciphers, instead of releasing the timings (*i.e.* latency) of the candidates.

4 Software Optimisations

For some ciphers software-optimised implementations are provided. These optimisations are achieved by the usage of architecture-specific instructions and intrinsics. An intrinsic function is handled in a special manner by the compiler where the intrinsic function maps to some specific assembler instructions. Table 4 gives an overview of the mainly used instruction set extensions in the 2nd round candidates. Furthermore, in the following we give a short overview of the most common used instruction set extensions to achieve software optimised algorithms.

4.1 AES-NI.

As many CAESAR candidates are AES based, they can obtain an increase in software performance by using the AES New Instructions [Gue12]. These set of instructions are available beginning with the 2010 Intel processors based on the 32nm microarchitecture Westmere. The instruction set consists of six instructions that offer full hardware support for AES enabling fast and secure encryption and decryption. The AES New Instructions increase the performance by more than an order of magnitude for parallel modes (*e.g.* CTR mode), and provide roughly 2-3 fold gains for non-parallelisable modes (*e.g.* CBC mode). On a Westmere microarchitecture the AES-NI instructions can run with approximately 1.3 cycles per byte in parallel mode of operation.

[§]<http://netsekure.org/2010/03/tls-overhead>

4.2 SSE.

The Streaming SIMD Extensions [Sie09] contain around 70 instructions for high performance optimised implementations. The SSE instructions are available since Pentium III and the latest update SSE4.2 is available with the Nehalem microarchitecture. The extensions provide up to 16 128-bit registers (xmm0-15) and provide vector-mode operations, enabling parallel execution of one operation on multiple data. The speedup that can be achieved with the SSE instructions depends on whether the data can be parallelised, as operations are used in a vector-mode where the same operation is executed on multiple data.

4.3 AVX.

The Advanced Vector Extensions [Lom11] were introduced with the Sandy Bridge microarchitecture and extend the SSE instructions with a new set of instructions and a new coding scheme. The AVX1 instructions extend the previous xmm0-15 128-bit registers to 16 256-bit registers (ymm0-15). Furthermore, memory alignments have been relaxed and three-operand non-destructive operations have been added. Previously, with two-operand commands the source operand was always overwritten by the instruction (*e.g.* $A = A + B$). With the new three-operand instructions (*e.g.* $A = B + C$) an additional `mov` instruction to secure the source-value is not necessary. Additionally, the AVX2 [Bux11] instructions are an advancement of the AVX instructions supporting integer datatypes and adding vector shift operations. The new instructions were introduced with the Haswell microarchitecture.

4.4 NEON.

The implementation of the Advanced SIMD extensions used in ARM processors is called NEON [neo] and is available with the Cortex-A microarchitecture. ARM processors are used in many mobile devices such as tablets and mobile phones. The NEON instructions are 128-bit SIMD extensions providing a flexible and powerful acceleration as they perform packaged SIMD processing. Registers are therefore considered as vectors of elements with the same data type and perform the same operation on all lanes.

5 Results

In the following, we present the results of the benchmarking of the 2nd round CAESAR candidates using our previously described framework. In this section, we illustrate a general overview of the best currently available implementations (*i.e.* software optimised versions, where applicable). In the appendices, we give a more detailed overview for each candidate. These illustrations comprise a 2d plot of any software implementation (*i.e.* several software optimised versions, where applicable), a 3d plot and a bar plot supporting our measurement settings for the best software optimised version of said candidate.

Figure 1 and Figure 2 gives a comparison of the best implementations for each CEASAR candidate on SandyBridge and Skylake processor, respectively. These graphs serve as an overview of the current best implementation with regards to latency. Moreover, Figure 7 illustrates a comparison between the best block cipher based candidates; Figure 8 a comparison of stream cipher based; Figure 9 a comparison of sponge based; Figure 10 a comparison of permutation based; and Figure 11 a comparison of compression function based candidates. In all graphs, we include a measurement of GCM as a baseline — which software optimised versions of the candidates should aim to reach or surpass. To demonstrate the impact of a CAESAR candidate in a real-world setting, we also made benchmarks in the following settings: Figure 3 compares the best implementation per

CAESAR candidate for a TLS setting on the Skylake architecture, while Figure 4 shows the same setting on the SandyBridge architecture. We chose the TLS setting, because we believe it is the most common usecase for authenticated encryption. Therefore, we set the associated data length to 5 bytes[¶] which represents the typical length of a TLS header. The message length is set to 1500 bytes, which corresponds to the MTU size of an ethernet frame. Moreover, we also made benchmarks for the SSH setting. In this setting, we fix the associated data length to 5 bytes and the message length to 1 byte (*i.e.* one key stroke). Figure 5 compares the best implementation per CAESAR candidate for the SSH setting on the Skylake architecture, and Figure 6 shows the same setting on the SandyBridge architecture. Furthermore, we created benchmarks for all candidates with increasing message/associated data lengths given in the appendices. Additionally, 3D plots are provided for the best implementation of each cipher, in order to illustrate the evolution in performance when the message length and the associated data length increase. We give detailed illustrations of these benchmarks in the appendices.

The benchmarking framework and our scripts to visualise the results are available online^{||} for reviewing purposes and to encourage other designers and researchers to use our framework for benchmarking their cryptographic schemes.

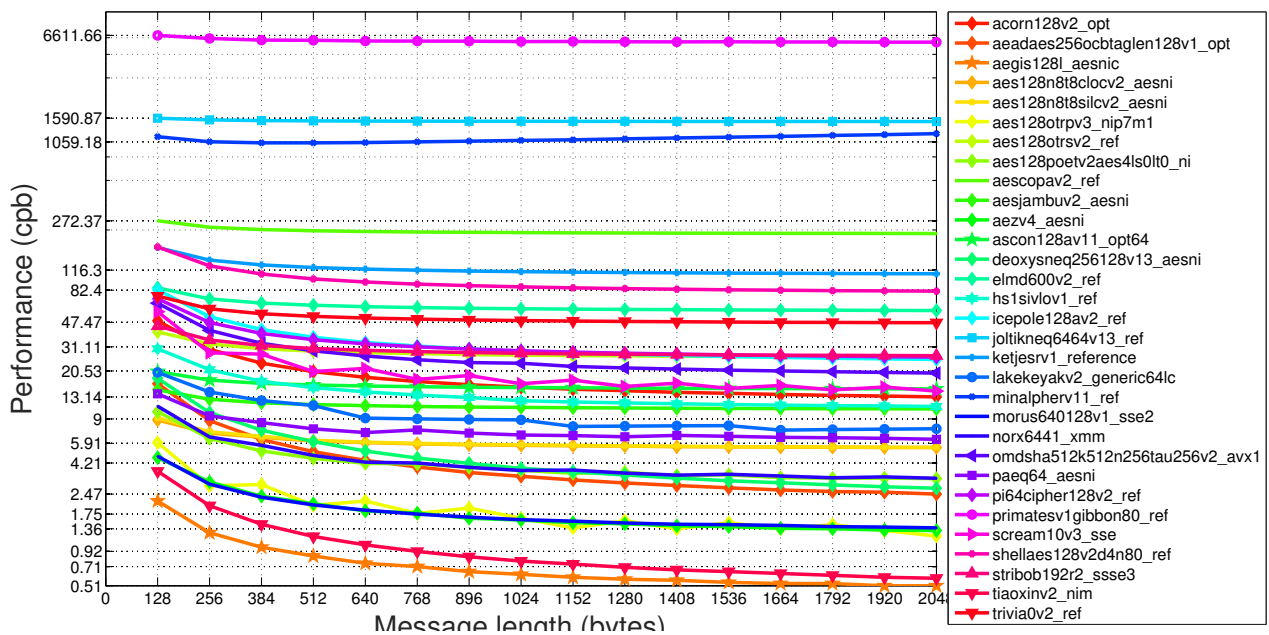


Figure 1: Comparison of the best implementation (on the SandyBridge processor) for each CAESAR candidate. The associated data is fixed to 0 bytes.

[¶]<http://netsekure.org/2010/03/tls-overhead>

^{||}https://github.com/TheBananaMan/caesar_benchmarks_secondround

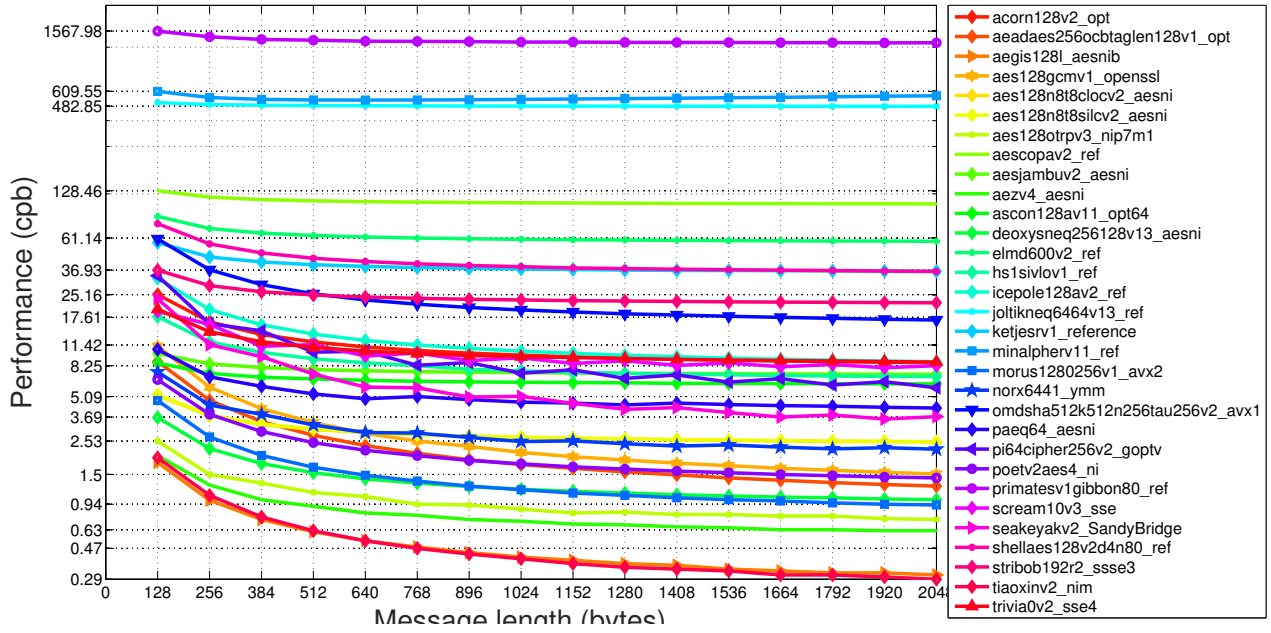


Figure 2: Comparison of the best implementation (on the SkyLake processor) for each CAESAR candidate. The associated data is fixed to 0 bytes.

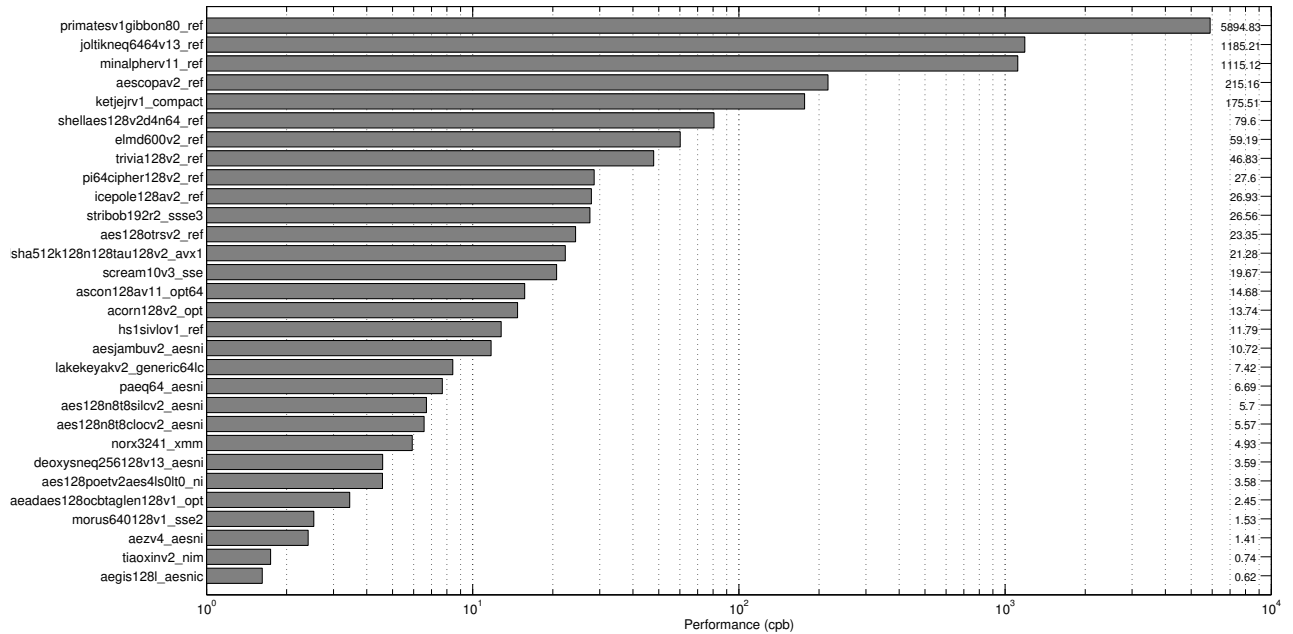


Figure 3: Comparison of 2nd round CAESAR candidates in the TLS setting (on the SandyBridge processor).

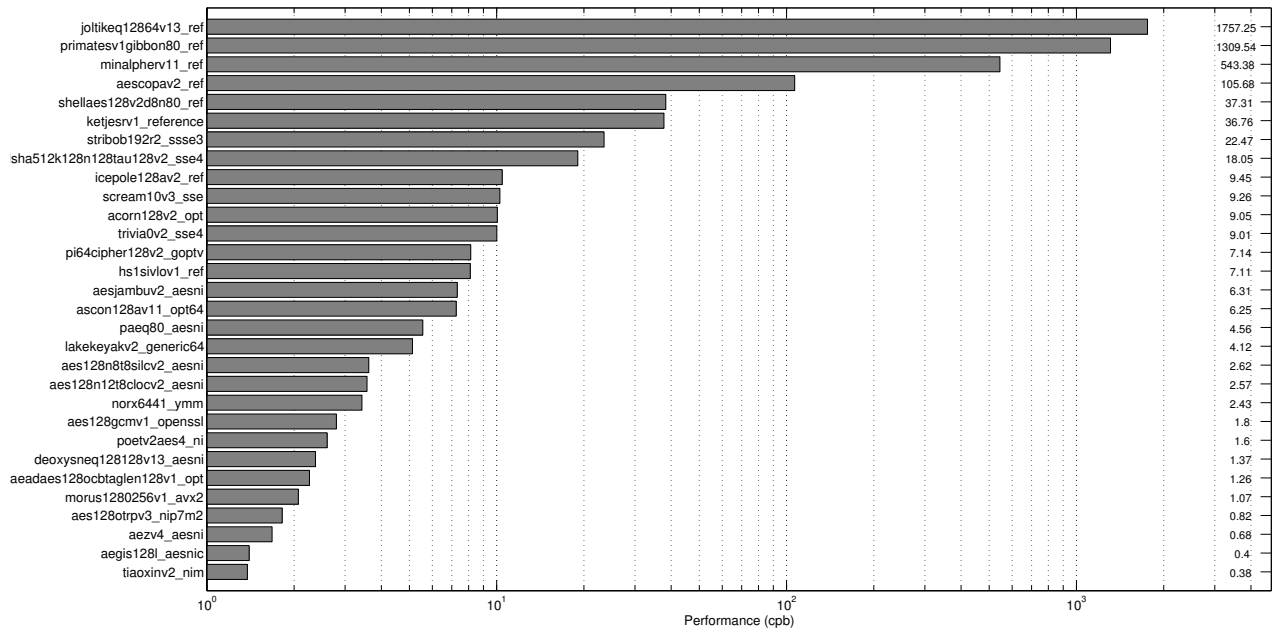


Figure 4: Comparison of 2nd round CAESAR candidates in the TLS setting (on the SkyLake processor).

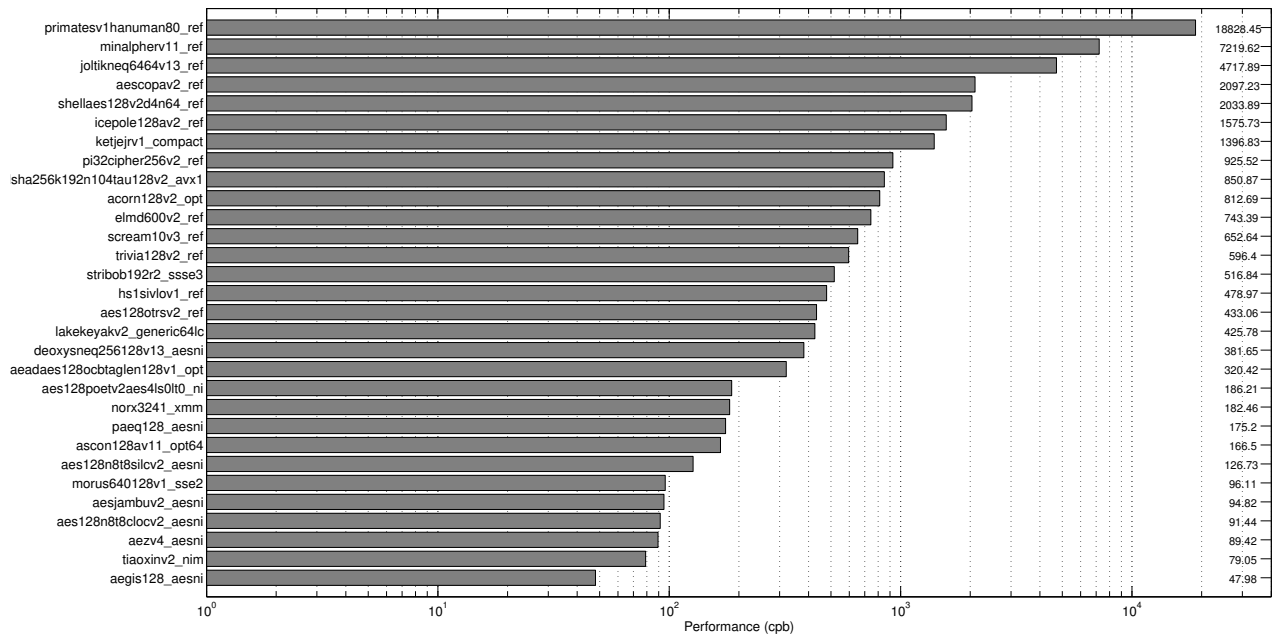


Figure 5: Comparison of 2nd round CAESAR candidates in the SSH setting (on the SandyBridge processor).

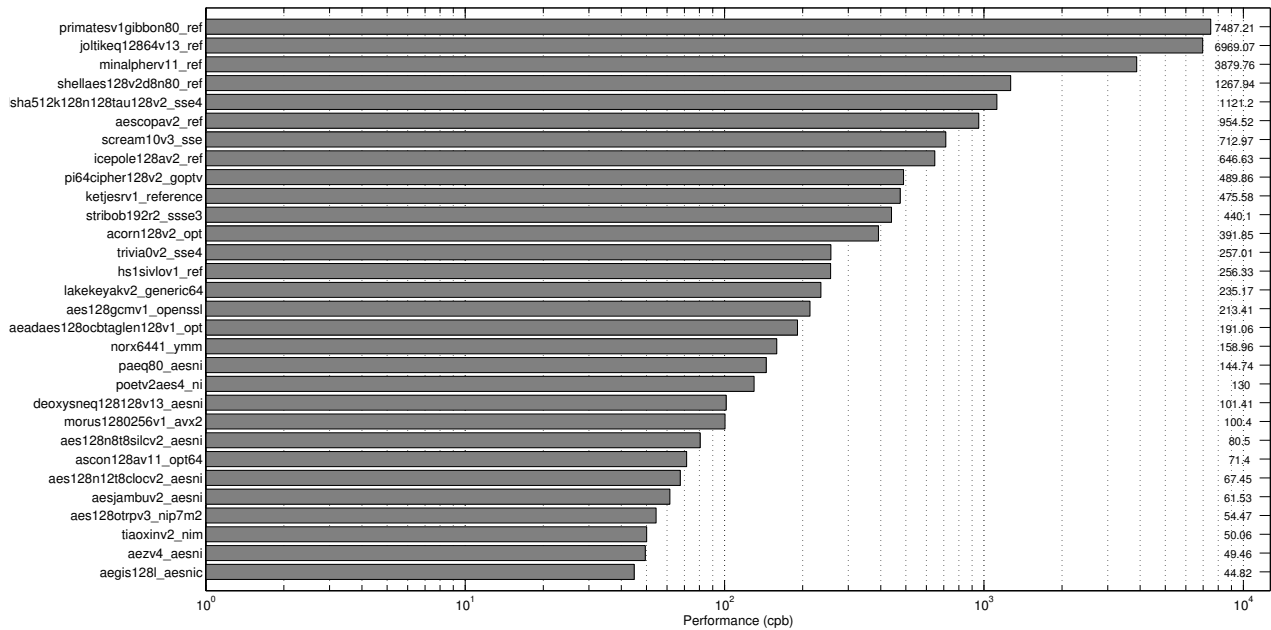


Figure 6: Comparison of 2nd round CAESAR candidates in the SSH setting (on the SkyLake processor).

6 Conclusion

In this paper, we present a new benchmarking framework to perform software performance measurements of authenticated encryption schemes. We apply our framework to benchmark the 2nd round CAESAR candidates. Software performance is an important factor in real-world applications. Our benchmarks show that candidates supported by a software-optimised implementation achieve a huge speedup with regards to others, without an optimised implementation. The aim of the CAESAR competition is to provide a portfolio of authenticated encryption algorithms, including implementations optimised for software (and hardware), as in the eStream portfolio [est08]. Currently, nearly two thirds of the candidates are supported by one or more software optimisations. Nevertheless, with our benchmarks we want to encourage designers to increase the number of optimised implementations.

Acknowledgements

We would like to thank the designers of the CAESAR candidates, which supported us with their software implementations. The first author is supported by the Marie Skłodowska-Curie ITN ECRYPT-NET grant (Project Reference 643161).

References

- [ABB⁺14] Elena Andreeva, Begül Bilgin, Andrey Bogdanov, Atul Luykx, Florian Mendel, Bart Mennink, Nicky Mouha, Qingju Wang, and Kan Yasuda. PRIMATES v1.02. <https://competitions.cr.ypt.to/round2/primatesv102.pdf>, 2014.

- [ABL⁺15] Elena Andreeva, Andrey Bogdanov, Atul Luykx, Bart Mennink, Elmar Tischhauser, and Kan Yasuda. AES-COPA v.2. <https://competitions.cr.yp.to/round2/aescopav2.pdf>, 2015.
- [AFF⁺15] Farzaneh Abed, Scott R. Fluhrer, John Foley, Christian Forler, Eik List, Stefan Lucks, David McGrew, and Jakob Wenzel. The POET Family of On-Line Authenticated Encryption Schemes. <https://competitions.cr.yp.to/round2/poetv20.pdf>, 2015.
- [AFL14] Farzaneh Abed, Christian Forler, and Stefan Lucks. General Overview of the Authenticated Schemes for the First Round of the CAESAR Competition. Cryptology ePrint Archive, Report 2014/792, 2014.
- [AJN15] Jean-Philippe Aumasson, Philipp Jovanovic, and Samuel Neves. NORX v2.0. <https://competitions.cr.yp.to/round2/norxv20.pdf>, 2015.
- [BDP⁺14] Guido Bertoni, Joan Daemen, Michaël Peeters, Gilles Van Assche, and Ronny Van Keer. CAESAR submission: KETJE v1. <https://competitions.cr.yp.to/round1/ketjev1.pdf>, 2014.
- [BDP⁺15] Guido Bertoni, Joan Daemen, Michaël Peeters, Gilles Van Assche, and Ronny Van Keer. CAESAR submission: KEYAK v2. <https://competitions.cr.yp.to/round2/keyakv21.pdf>, 2015.
- [Ber14] Daniel J. Bernstein. Caesar: Competition for authenticated encryption: Security, applicability, and robustness. <https://competitions.cr.yp.to/caesar.html>, 2014.
- [Ber16] Daniel J. Bernstein. Supercop. <https://bench.cr.yp.to/supercop.html>, 2016.
- [BK14] Alex Biryukov and Dmitry Khovratovich. PAEQ v1. <https://competitions.cr.yp.to/round1/paeqv1.pdf>, 2014.
- [Bux11] Mark Buxton. Intel[®] advanced vector extensions programming reference. <https://software.intel.com/en-us/blogs/2011/06/13/haswell-new-instruction-descriptions-now-available>, 2011.
- [CHVV03] Brice Canvel, Alain Hiltgen, Serge Vaudenay, and Martin Vuagnoux. *Password Interception in a SSL/TLS Channel*, pages 583–599. Springer, 2003.
- [CM15] Avik Chakraborti and Nandi Mridul. TriviA-ck-v2. <https://competitions.cr.yp.to/round2/triviackv2.pdf>, 2015.
- [CMN⁺15] Simon Cogliani, Diana Maimuk, David Naccache, Rodrigo Portella, Reza Reyhanitabar, Serge Vaudenay, and Damian Vizár. Offset Merkle-Damgård (OMD) version 2.0. <https://competitions.cr.yp.to/round2/omdv20.pdf>, 2015.
- [DEMS15] Christoph Dobraunig, Maria Eichlseder, Florian Mendel, and Martin Schläffer. ASCON v1.1. <https://competitions.cr.yp.to/round2/asconv11.pdf>, 2015.
- [DN15] Nilanjan Datta and Mridul Nandi. ELmD v2.0. <https://competitions.cr.yp.to/round2/elmdv20.pdf>, 2015.
- [est08] estream: the ecrypt stream cipher project. <http://www.ecrypt.eu.org/stream/>, 2008.

- [GLS⁺15] Vincent Grosso, Gaëtan Leurent, François-Xavier Standaert, Kerem Varici, Anthony Journault, François Durvaux, Lubos Gaspar, and Stephanie Kerckhof. SCREAM: Side-Channel Resistant Authenticated Encryption with Masking. <https://competitions.cr.yt.to/round2/screamv3.pdf>, 2015.
- [GMS⁺15] Danilo Gligoroski, Hristina Mihajloska, Simona Samardjiska, Håkon Jacobsen, Mohamed El-Hadedy, Rune Erlend Jensen, and Daniel Otte. π -cipher v2.0. <https://competitions.cr.yt.to/round2/picipherv20.pdf>, 2015.
- [Gue12] Shay Gueron. Intel[®] advanced encryption standard (aes) new instructions set. Technical report, Intel Corporation, 2012.
- [HDF⁺15] Ekawat Homsirikamol, William Diehl, Ahmed Ferozpuri, Farnoud Farahmand, Malik Umar Sharif, and Kris Gaj. GMU Hardware API for Authenticated Ciphers. Cryptology ePrint Archive, Report 2015/669, 2015.
- [HKR15] Viet Tung Hoang, Ted Krovetz, and Phillip Rogaway. AEZ v4.1: Authenticated Encryption by Enciphering. <https://competitions.cr.yt.to/round2/aezv41.pdf>, 2015.
- [HW15] Tao Huang and Hongjun Wu. The Authenticated Cipher MORUS (v1). <https://competitions.cr.yt.to/round2/morusv11.pdf>, 2015.
- [IMG⁺15] Tetsu Iwata, Kazuhiko Minematsu, Jian Guo, Sumio Morioka, and Eita Kobayashi. SILC: Simple Lightweight CFB. <https://competitions.cr.yt.to/round2/silcv2.pdf>, 2015.
- [IMGM15] Tetsu Iwata, Kazuhiko Minematsu, Jian Guo, and Sumio Morioka. CLOC: Compact Low-Overhead CFB. <https://competitions.cr.yt.to/round2/clocv2.pdf>, 2015.
- [JNP15a] Jérémy Jean, Ivica Nikolić, and Thomas Peyrin. Deoxys v1.3. <https://competitions.cr.yt.to/round2/deoxysv13.pdf>, 2015.
- [JNP15b] Jérémy Jean, Ivica Nikolić, and Thomas Peyrin. Joltik v1.3. <https://competitions.cr.yt.to/round2/joltikv13.pdf>, 2015.
- [KR11] Ted Krovetz and Phillip Rogaway. *The Software Performance of Authenticated-Encryption Modes*, pages 306–327. Springer, 2011.
- [KR14] Ted Krovetz and Phillip Rogaway. OCB (v1). <https://competitions.cr.yt.to/round1/ocbv1.pdf>, 2014.
- [Kro15] Ted Krovetz. HS1-SIV (v2). <https://competitions.cr.yt.to/round2/hs1sivv2.pdf>, 2015.
- [Lom11] Chris Lomont. Introduction to intel[®] advanced vector extensions. <https://software.intel.com/en-us/articles/introduction-to-intel-advanced-vector-extensions>, 2011.
- [MGH⁺15] Paweł Morawiecki, Kris Gaj, Ekawat Homsirikamol, Krystian Matusiewicz, Josef Pieprzyk, Marcin Rogawski, Marian Srebrny, and Marcin Wójcik. ICE-POLE v2. <https://competitions.cr.yt.to/round2/icepolev2.pdf>, 2015.
- [Min16] Kazuhiko Minematsu. AES-OTR v3. <https://competitions.cr.yt.to/round2/aesotrv3.pdf>, 2016.
- [neo] Neon.

- [Nik15] Ivica Nikolić. Tiaoxin-346. <https://competitions.cr.yj.to/round2/tiaoxinv2.pdf>, 2015.
- [OSB15] Markku-Juhani O. Sarrinen and Billy B. Brumley. STRIBOBr2: "WHIRLBOB". <https://competitions.cr.yj.to/round2/stribobr2.pdf>, 2015.
- [Pao10] Gabriele Paoloni. How to benchmark code execution times on intel[®] ia-32 and ia-64 instruction set architectures. Technical report, Intel Corporation, 2010.
- [Saa16] Markku-Juhani Saarinen. The BRUTUS automatic cryptanalytic framework. *Journal of Cryptographic Engineering*, 6(1):75–82, 2016.
- [Sie09] Sam Siewert. Using Intel[®] Streaming SIMD Extensions and Intel[®] Integrated Performance Primitives to Accelerate Algorithms. <https://software.intel.com/en-us/articles/using-intel-streaming-simd-extensions-and-intel-integrated-performance-primitives-to-accelerate-algorithms>, 2009.
- [STA⁺15] Yu Sasaki, Yosuke Todo, Kazumaro Aoki, Yusuke Naito, Takeshi Sugawara, Yumiko Murakami, Mitsuru Matsui, and Shoichi Hirose. Minalpher v1.1. <https://competitions.cr.yj.to/round2/minalpherv11.pdf>, 2015.
- [Vau02] Serge Vaudenay. *Security Flaws Induced by CBC Padding — Applications to SSL, IPSEC, WTLS...*, pages 534–545. Springer, 2002.
- [Wan15] Lei Wang. SHELL v2.0. <https://competitions.cr.yj.to/round2/shellv20.pdf>, 2015.
- [WH15] Hongjun Wu and Tao Huang. The JAMBU Lightweight Authentication Encryption Mode (v2). <https://competitions.cr.yj.to/round2/aesjambuv2.pdf>, 2015.
- [WP14] Hongjun Wu and Bart Preneel. AEGIS: A Fast Authenticated Encryption Algorithm (v1). <https://competitions.cr.yj.to/round1/aegisv1.pdf>, 2014.
- [Wu15] Hongjun Wu. ACORN: a Lightweight Authenticated Cipher (vs). <https://competitions.cr.yj.to/round2/acornv2.pdf>, 2015.

A Comparison of Candidates per Type

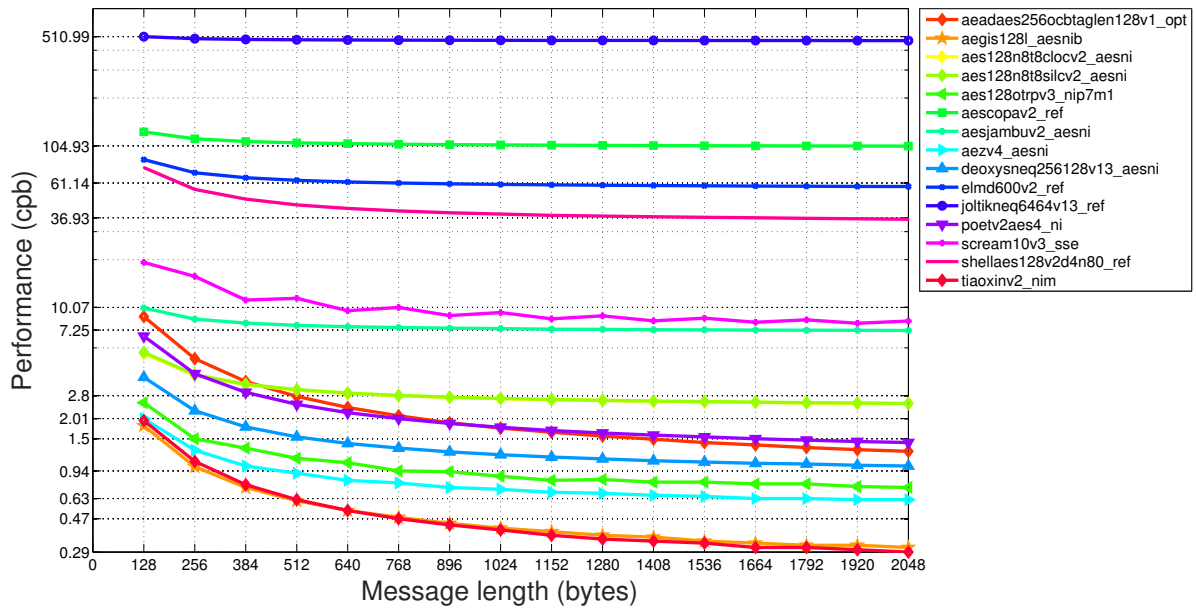


Figure 7: Comparison of Block cipher based 2nd round CAESAR candidates

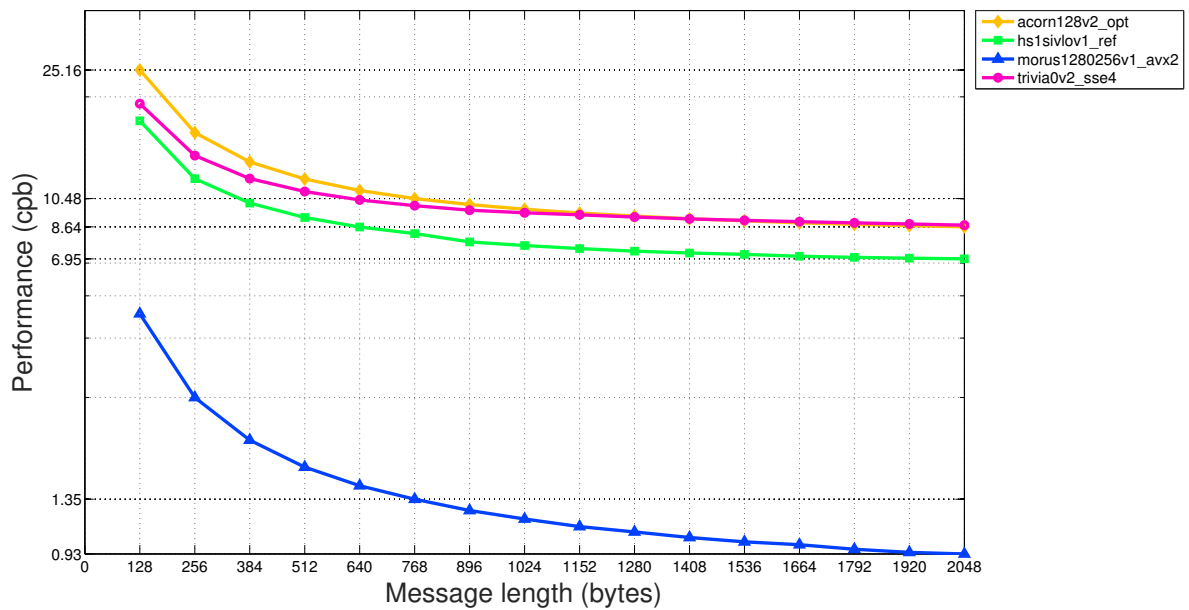


Figure 8: Comparison of Stream cipher based 2nd round CAESAR candidates

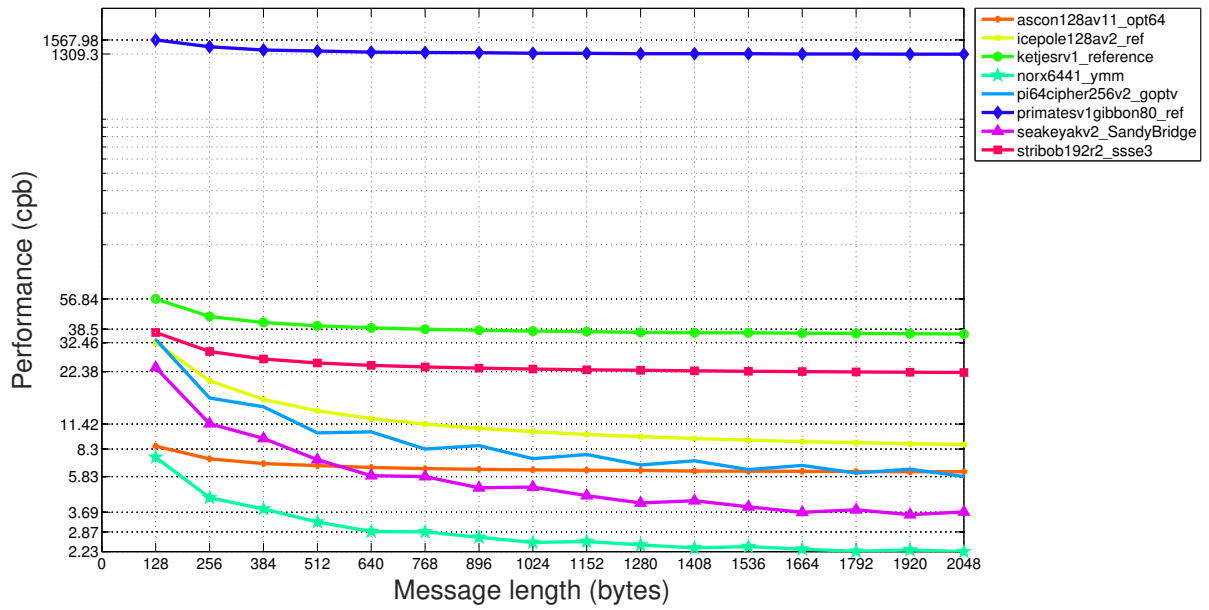


Figure 9: Comparison of Sponge based 2nd round CAESAR candidates

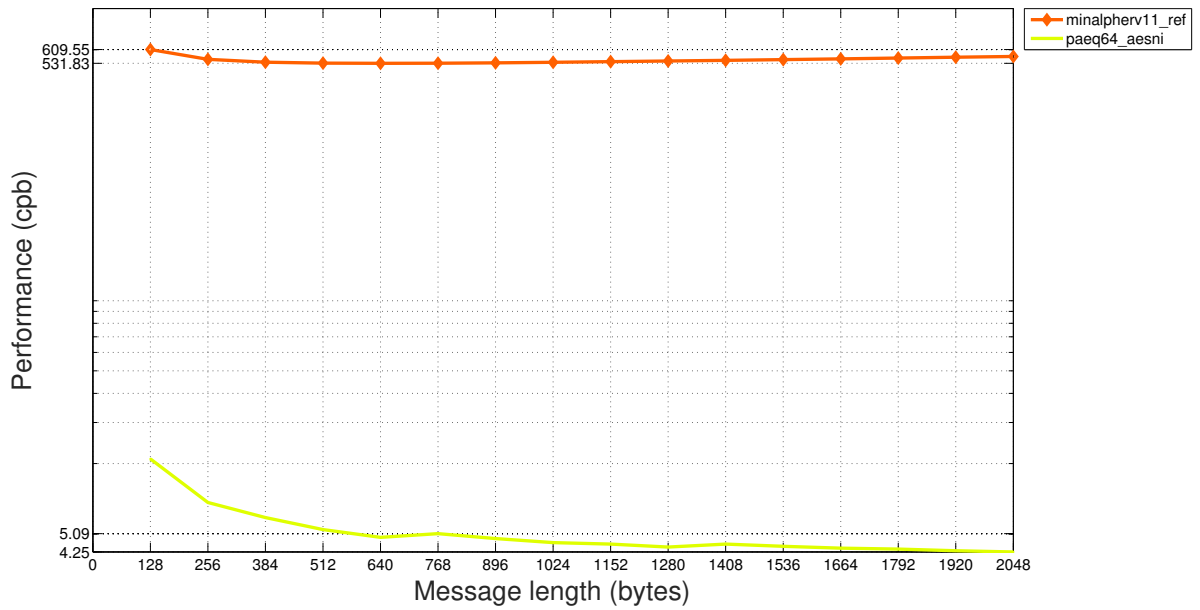


Figure 10: Comparison of Permutation based 2nd round CAESAR candidates

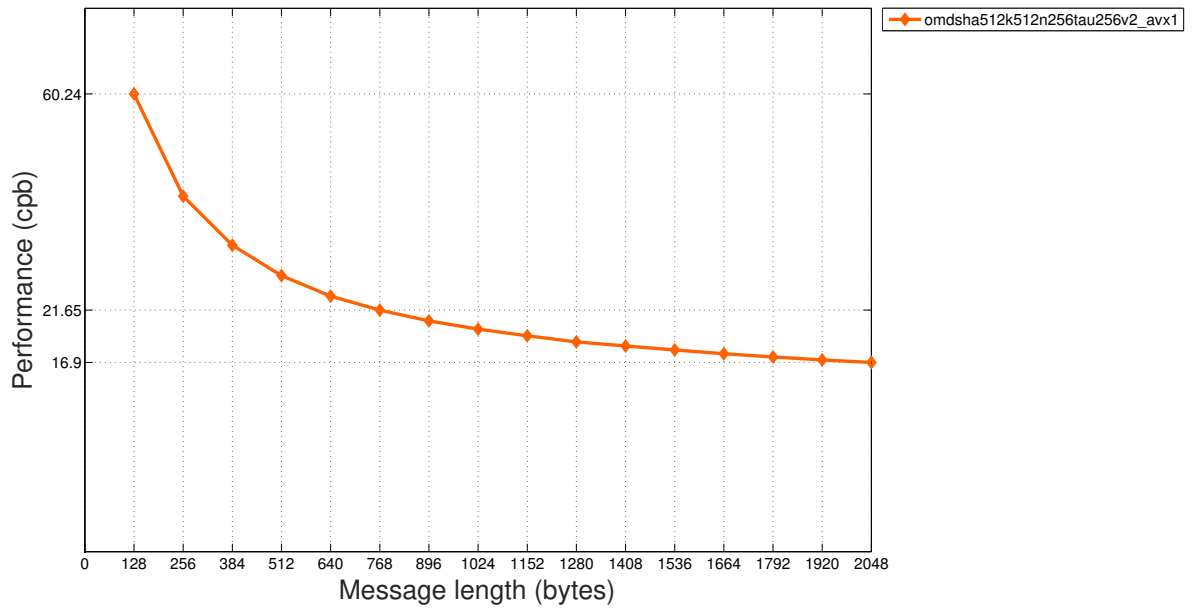


Figure 11: Comparison of Compression function based 2nd round CAESAR candidates

B Comparison of all Implementations per Candidate

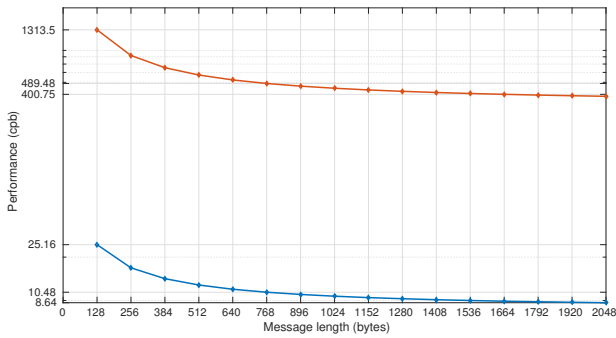


Figure 12: acorn128v2_opt (blue), acorn128v2_ref (orange)

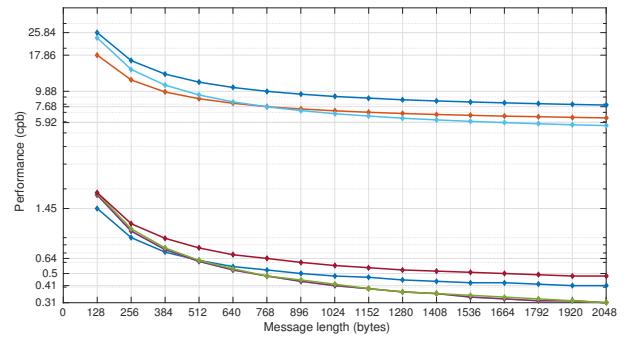


Figure 13: aegis128_aesni (blue), aegis128_ref (orange), aegis128l_aesnia (yellow), aegis128l_aesnib (brown), aegis128l_aesnic (green), aegis128l_ref (light blue), aegis256_aesni (purple), aegis256_ref (darkblue)

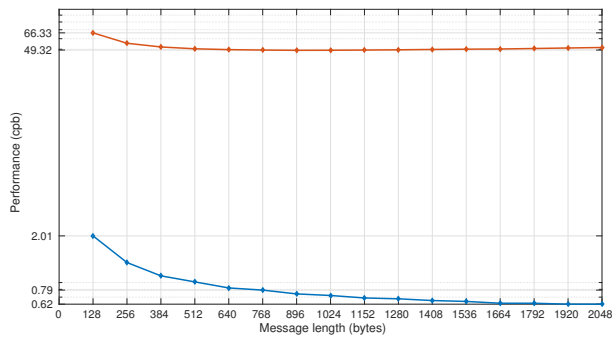


Figure 14: aezv4_aesni (blue), aezv4_ref (orange)

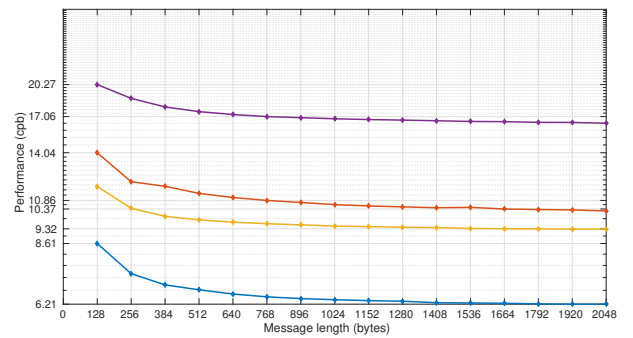


Figure 15: ascon128av11_opt64 (blue), ascon128av11_ref (orange), ascon128v11_opt64 (yellow), ascon128v11_ref (purple)

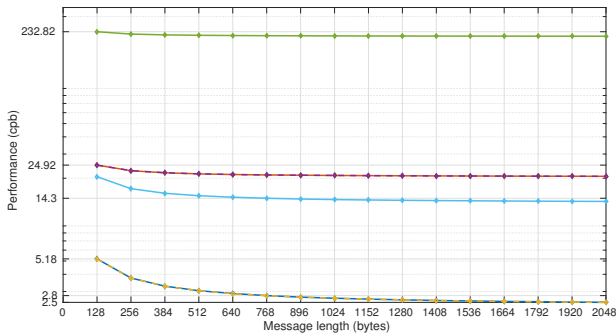


Figure 16: aes128n12t8clocv2_aesni (blue), aes128n12t8clocv2_ref (orange), aes128n8t8clocv2_aesni (yellow), aes128n8t8clocv2_ref (purple), twine80n6t4clocv2_ref (green), twine80n6t4clocv2_vperm (light blue)

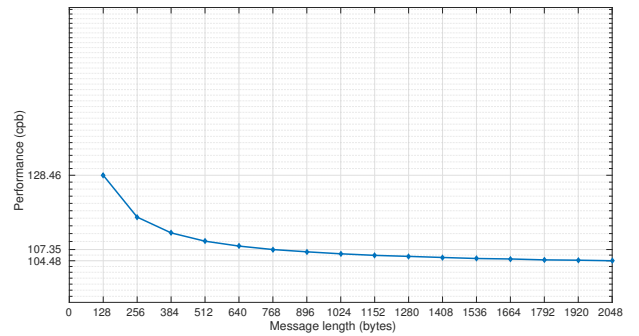


Figure 17: aescopav2_ref (blue)

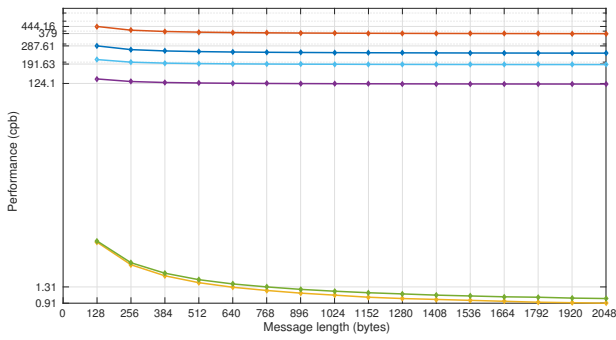


Figure 18: deoxyseq128128v13_ref (blue), deoxyseq256128v13_ref (orange), deoxysneq128128v13_aesni (yellow), deoxysneq128128v13_ref (purple), deoxysneq256128v13_aesni (light blue), deoxysneq256128v13_ref (cyan)

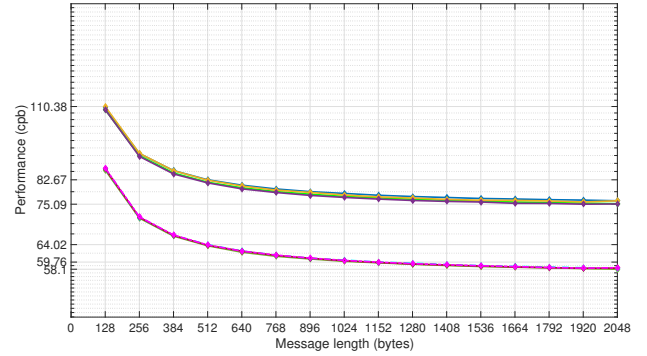


Figure 19: elmd1000v2_ref (blue), elmd1001v2_ref (green), elmd101270v2_ref (yellow), elmd101271v2_ref (purple), elmd600v2_ref (green), elmd601v2_ref (cyan dotted), elmd61279v2_ref (magenta), elmd61271v2_ref (purple dotted)

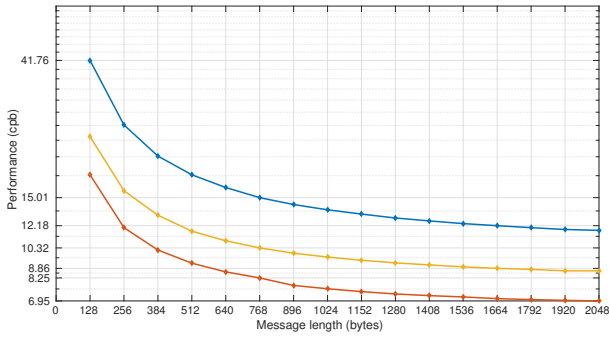


Figure 20: hs1sivhiv1_ref (blue), hs1sivlv1_ref (orange), hs1sivv1_ref (yellow)

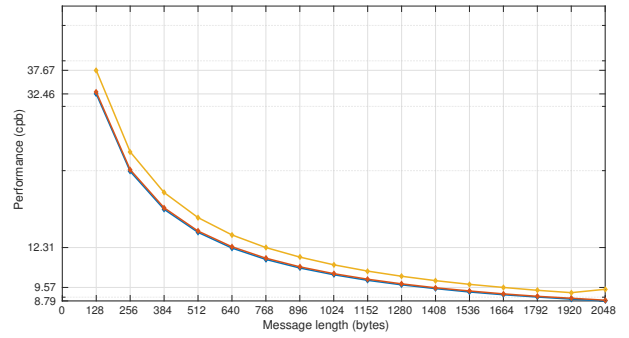


Figure 21: icepole128av2_ref (blue), icepole128v2_ref (orange), icepole256av2_ref (yellow)

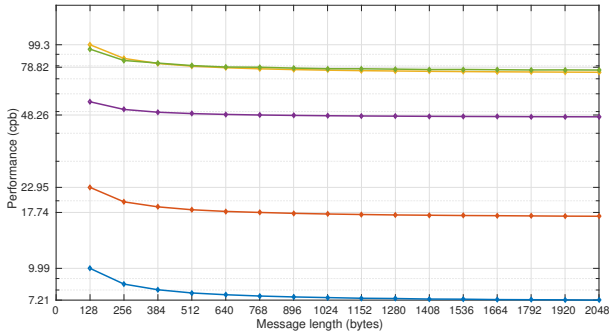


Figure 22: aesjambuv2_aesni (blue), aesjambuv2_ref (orange), simonjambu128v2_ref (yellow), simonjambu64v2_ref (purple), simonjambu96v2_ref (green)

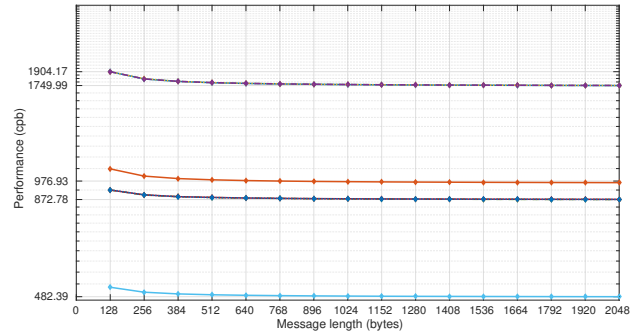


Figure 23: joltikeq12864v13_ref (light green), joltikeq6464v13_ref (orange), joltikeq80112v13_ref (yellow), joltikeq9696v13_ref (purple), joltikneq12864v13_ref (green), joltikneq6464v13_ref (light blue), joltikneq80112v13_ref (magenta), joltikneq9696v13_ref (blue)

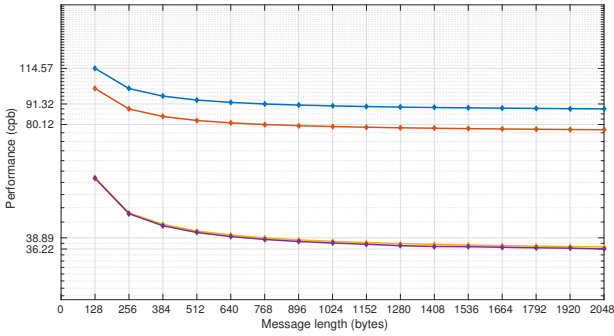


Figure 24: ketjesrv1_compact (blue), ketjesrv1_reference (orange), ketjesrv1_compact (yellow), ketjesrv1_reference (purple)

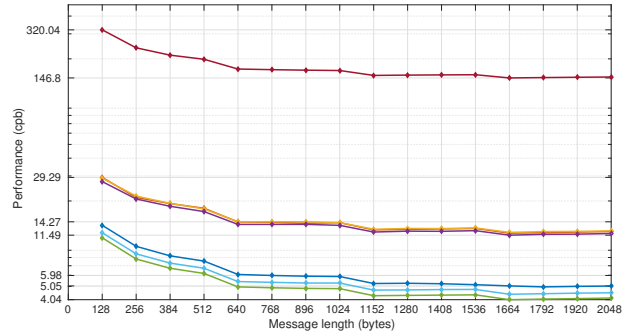


Figure 25: lakekeyakv2_reference32bit (magenta), lakekeyakv2_compact (red), lakekeyakv2_generic32 (yellow), lakekeyakv2_generic32lc (purple), lakekeyakv2_generic64 (green), lakekeyakv2_generic64lc (light blue), lakekeyakv2_SandyBridge (dark blue)

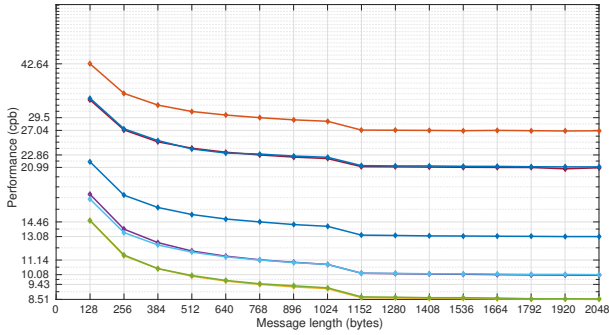


Figure 26: riverkeyakv2_compact (orange), riverkeyakv2_generic32 (yellow), riverkeyakv2_generic32lc (purple), riverkeyakv2_generic64 (purple), riverkeyakv2_generic64lc (light blue), riverkeyakv2_reference (brown), riverkeyakv2_reference32bits (dark blue), riverkeyakv2_SandyBridge (blue)

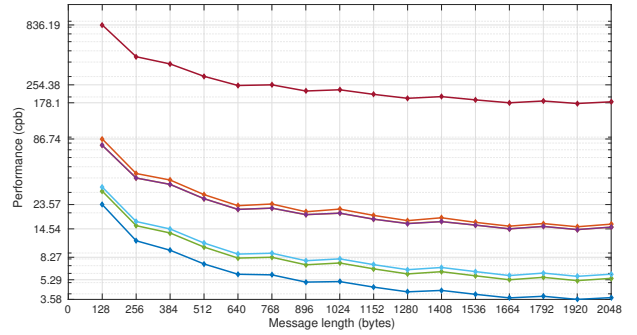


Figure 27: seakeyakv2_reference32bits (magenta), seakeyakv2_compact (orange), seakeyakv2_generic32 (yellow), seakeyakv2_generic32lc (purple), seakeyakv2_generic64 (green), seakeyakv2_generic64lc (light blue), seakeyakv2_SandyBridge (blue)

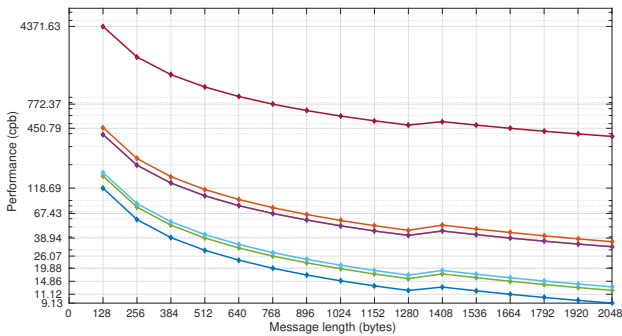


Figure 28: lunarkeyakv2_reference32bits (magenta), lunarkeyakv2_compact (orange), lunarkeyakv2_generic32 (yellow), lunarkeyakv2_generic32lc (purple), lunarkeyakv2_generic64 (green), lunarkeyakv2_generic64lc (light blue), lunarkeyakv2_SandyBridge (blue)

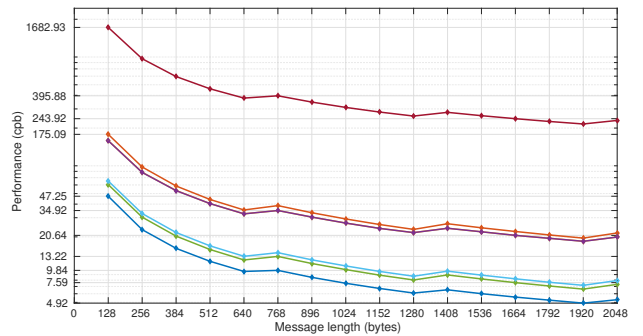


Figure 29: oceankeyakv2_reference32bits (magenta), oceankeyakv2_compact (orange), oceankeyakv2_generic32 (yellow), oceankeyakv2_generic32lc (purple), oceankeyakv2_generic64 (green), oceankeyakv2_generic64lc (light blue), oceankeyakv2_SandyBridge (blue)

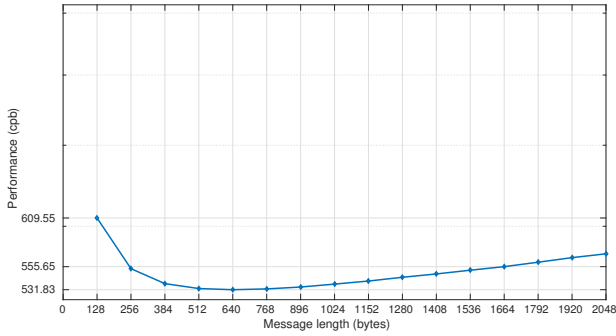


Figure 30: minalpherv11_ref (blue)

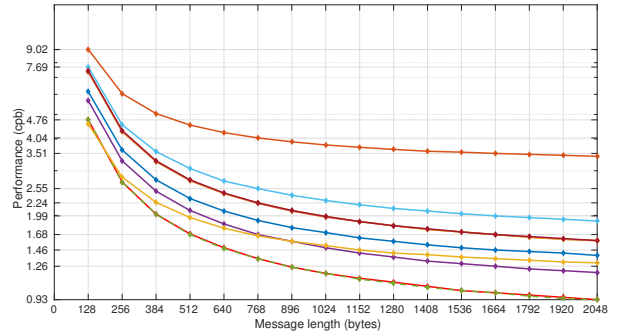


Figure 31: morus640128v1_ref (orange), morus1280256v1_ref (light blue), morus1280128v1_avx2 (red), morus1280128v1_ref64 (brown), morus1280256v1_ref64 (brown), morus1280128v1_ref (brown), morus1280256v1_avx2 (green dotted), morus1280256v1_sse2 (blue), morus6400128v1_sse2 (purple), morus1280128v1_sse2 (yellow)

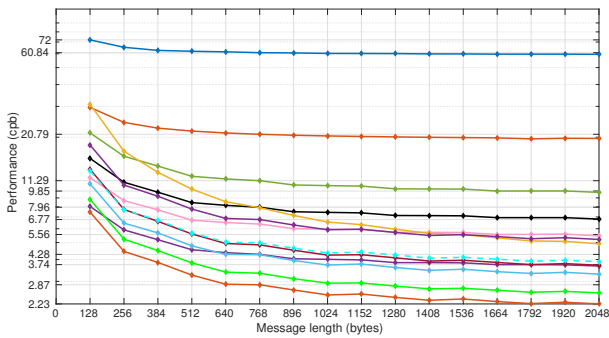


Figure 32: norx0841_ref (blue), norx1641_ref (orange), norx3241_ref (black), norx3241_xmm (purple), norx3261_ref (green), norx3261_xmm (pink), norx6441_ref (magenta), norx6441_ymm (brown), norx6441_xmm (light green), norx6444_ref (yellow), norx6461_ref (purple), norx6461_xmm (cyan dotted), norx6461_ymm (light blue)

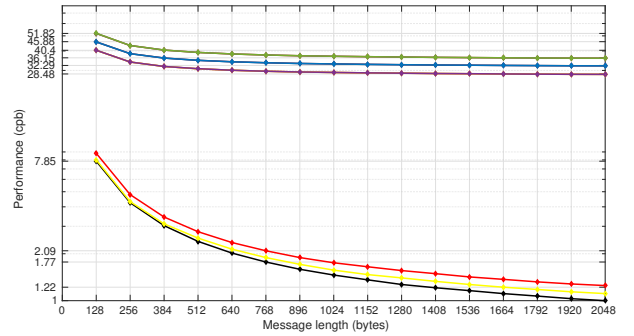


Figure 33: aes128ocbtaglen128v1_opt (black), aes128ocbtaglen128v1_ref (purple), aes128ocbtaglen64v1_ref (purple), aes128ocbtaglen96v1_ref (purple), aes192ocbtaglen128v1_opt (yellow), aes192ocbtaglen128v1_ref (blue), aes192ocbtaglen64v1_ref (blue), aes192ocbtaglen96v1_ref (blue), aes256ocbtaglen128v1_opt (red), aes256ocbtaglen128v1_ref (green), aes256ocbtaglen64v1_ref (green), aes256ocbtaglen96v1_ref (green)

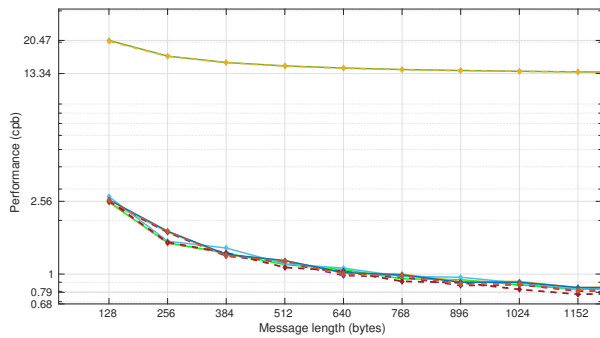


Figure 34: aes128otrsv3_ref (green), aes128otrsv3_ref (yellow), aes128otrsv3_nip7m1 (blue), aes128otrsv3_nip7m2 (magenta dotted), aes128otrsv3_nip8m1 (purple dotted), aes128otrsv3_nip8m2 (light green), aes128otrsv3_nip7m1 (light red dotted), aes128otrsv3_nip7m2 (magenta dotted), aes128otrsv3_nip8m1 (dark blue), aes128otrsv3_nip8m2 (light blue)

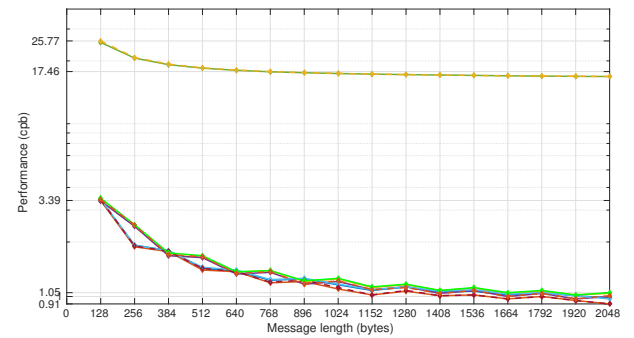


Figure 35: aes128otrsv3_ref (green), aes256otrsv3_ref (yellow), aes256otrsv3_nip7m1 (blue), aes256otrsv3_nip7m2 (magenta dotted), aes256otrsv3_nip8m1 (purple dotted), aes256otrsv3_nip8m2 (light green), aes256otrsv3_nip7m1 (light red dotted), aes256otrsv3_nip7m2 (magenta dotted), aes256otrsv3_nip8m1 (dark blue), aes256otrsv3_nip8m2 (light blue)

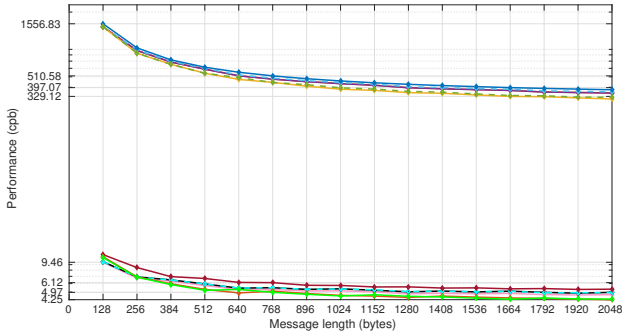


Figure 36: paeq128_aesni (pink), paeq128_ref (purple), paeq128t_aesni (black), paeq128t_ref (purple), paeq128tnm_aesni(cyan dotted), paeq128tnm_ref (light blue dotted), paeq160_aesni (magenta), paeq160_ref (blue), paeq64_aesni (brown), paeq64_ref (yellow), paeq80_aesni (light green), paeq80_ref (green dotted)

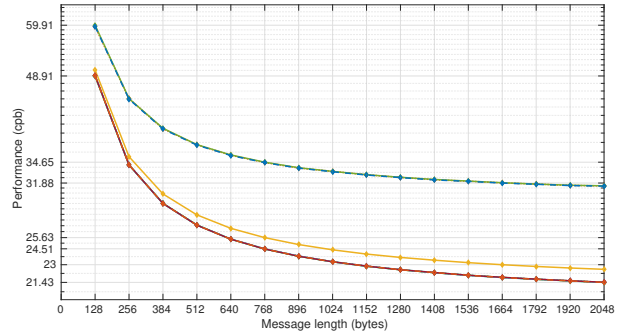


Figure 37: omdsha256k128n96tau128v2_avx1 (red), omdsha256k128n96tau128v2_ref (green dotted), omdsha256k128n96tau128v2_sse4 (yellow), omdsha256k128n96tau64v2_avx1 (purple), omdsha256k128n96tau64v2_ref (green dotted), omdsha256k128n96tau64v2_sse4 (red), omdsha256k128n96tau96v2_avx1 (purple), omdsha256k128n96tau96v2_ref (blue dotted), omdsha256k128n96tau96v2_sse4 (red)

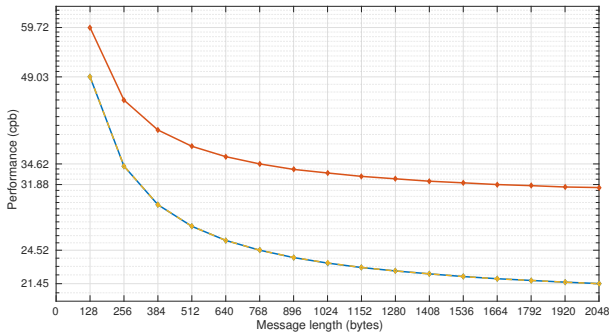


Figure 38: omdsha256k192n104tau128v2_avx1 (blue), omdsha256k192n104tau128v2_ref (orange), omdsha256k192n104tau128v2_sse4 (yellow dotted)

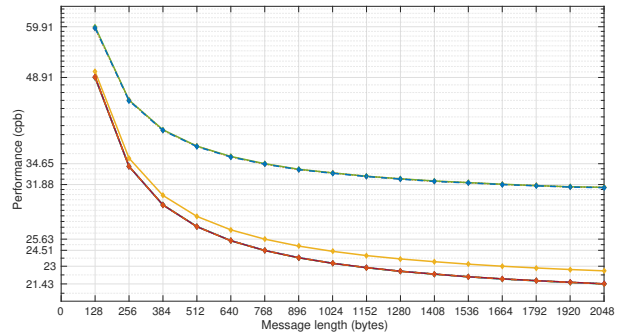


Figure 39: omdsha256k256n104tau160v2_avx1 (red dotted), omdsha256k256n104tau160v2_ref (blue), omdsha256k256n104tau160v2_sse4 (red dotted), omdsha256k256n248tau256v2_avx1 (yellow), omdsha256k256n248tau256v2_ref (green), omdsha256k256n248tau256v2_sse4 (purple)

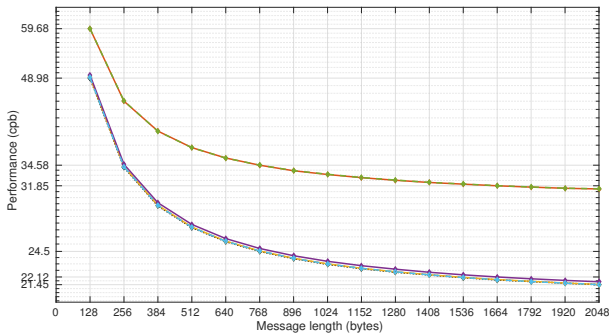


Figure 40: omdsha512k128n128tau128v2_avx1 (light blue dotted), omdsha512k128n128tau128v2_ref (red), omdsha512k128n128tau128v2_sse4 (purple dotted), omdsha512k256n256tau256v2_avx1 (yellow), omdsha512k256n256tau256v2_ref (green), omdsha512k256n256tau256v2_sse4 (purple), omdsha512k512n256tau256v2_avx1 (yellow), omdsha512k512n256tau256v2_ref (green), omdsha512k512n256tau256v2_sse4 (light blue dotted)

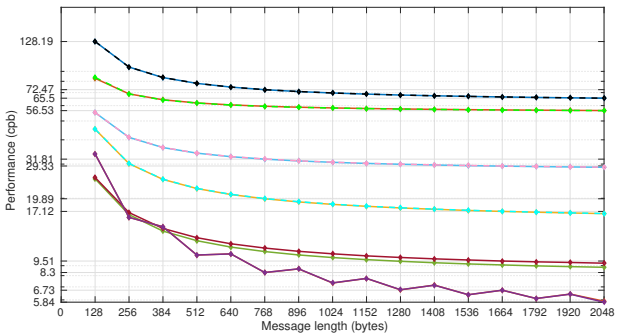


Figure 41: pi16cipher096v2_ref (red), pi16cipher128v2_ref (light green dotted), pi32cipher128v2_ref (pink dotted), pi32cipher256v2_ref (light gblue), pi64cipher128v2_ref (yellow), pi64cipher256v2_ref (cyan dotted), pi16cipher096v2_goptv (black dotted), pi16cipher128v2_goptv (blue), pi32cipher128v2_goptv (green), pi32cipher256v2_goptv (magenta), pi64cipher128v2_goptv (purple), pi64cipher256v2_goptv (purple)

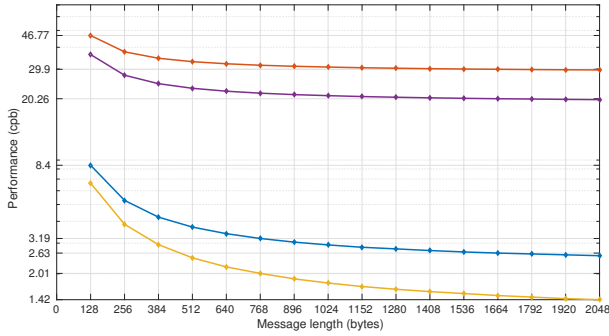


Figure 42: poeTV2AES128_ni (blue), poeTV2AES128_ref (orange), poeTV2AES4_ni (yellow) poeTV2AES4_ref (purple)

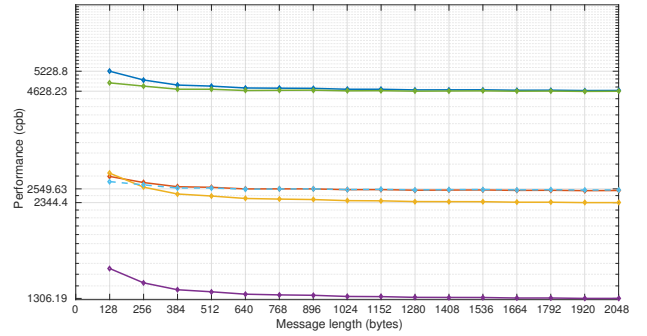


Figure 43: primatesV1ape120_ref (blue), primatesV1ape80_ref (orange), primatesV1gibbon120_ref (yellow), primatesV1gibbon80_ref (purple), primatesV1hanuman120_ref (green), primatesV1hanuman80_ref (cyan dotted)

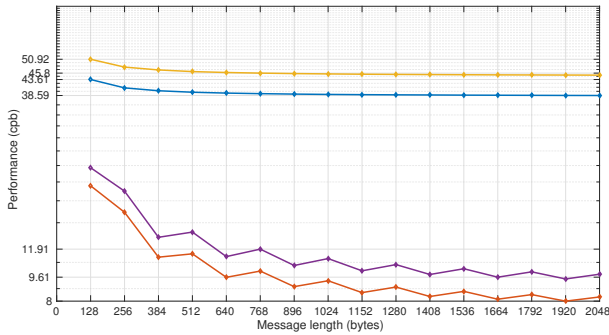


Figure 44: scream10v3_ref (blue), scream10v3_sse (orange), scream12v3_ref (yellow), scream12v3_sse (purple)

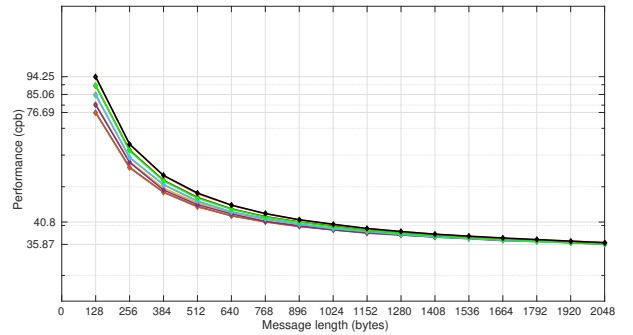


Figure 45: shellAES128v2d4n64_ref (red), shellAES128v2d4n80_ref (blue), shellAES128v2d5n64_ref (green), shellAES128v2d5n80_ref (purple), shellAES128v2d6n64_ref (yellow), shellAES128v2d6n80_ref (cyan), shellAES128v2d7n64_ref (light green), shellAES128v2d7n80_ref (purple), shellAES128v2d8n64_ref (orange), shellAES128v2d8n80_ref (black)

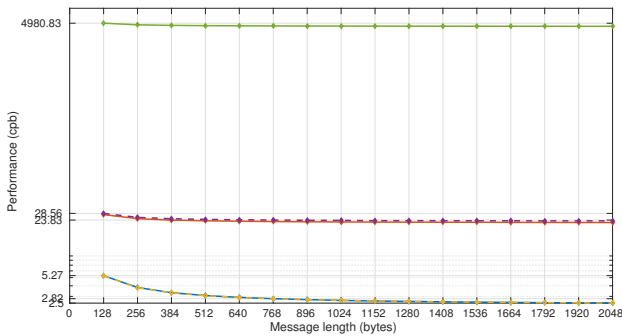


Figure 46: present80n6t4silcv2_ref (green), aes128n12t8silcv2_aesni (blue), aes128n12t8silcv2_ref (red), aes128n8t8silcv2_aesni (yellow), aes128n8t8silcv2_ref (purple)

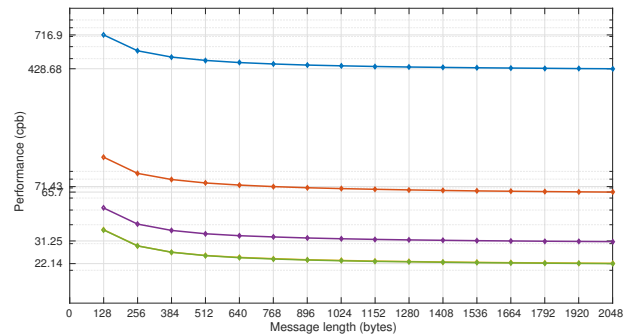


Figure 47: sTriBob192r2_8bit (blue), sTriBob192r2_bitslice (orange), sTriBob192r2_ref (yellow), sTriBob192r2_smaller (purple), sTriBob192r2_ssse3 (green)

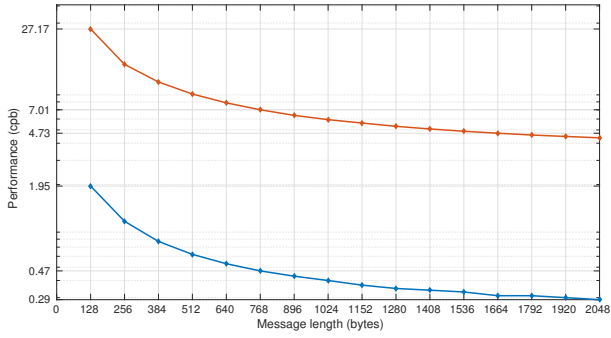


Figure 48: tiaoxinv2_nim (blue), tiaoxinv2_ref (orange)

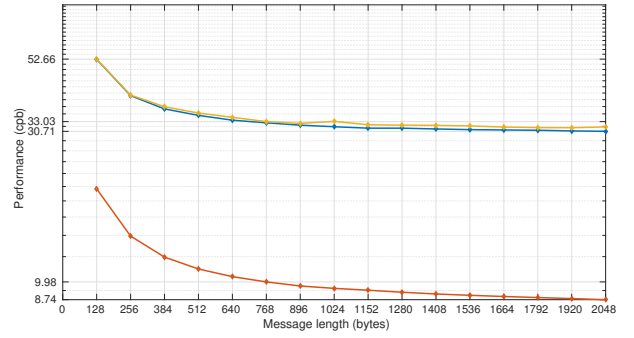


Figure 49: trivia0v2_ref (blue), trivia128v2_ref (yellow), trivia128v2_sse4 (orange)

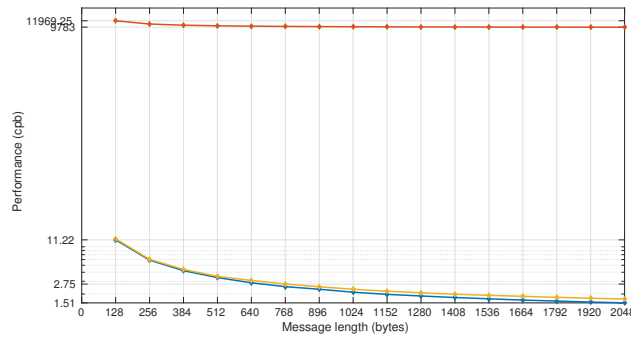


Figure 50: aesgcm128_ref (orange), aesgcm128_openssl (blue), aesgcm256_openssl (yellow)

C 3D Plots for Increasing Message and Associated Data Lengths

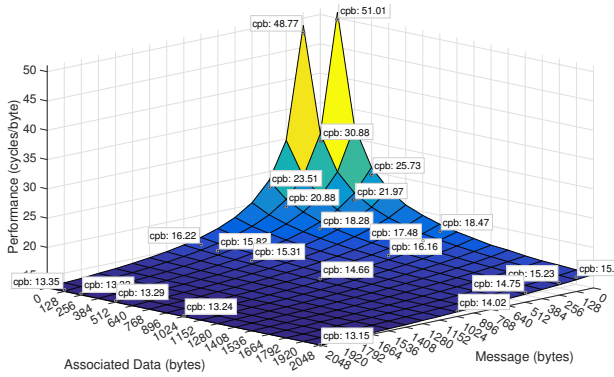


Figure 51: acorn128v2_opt

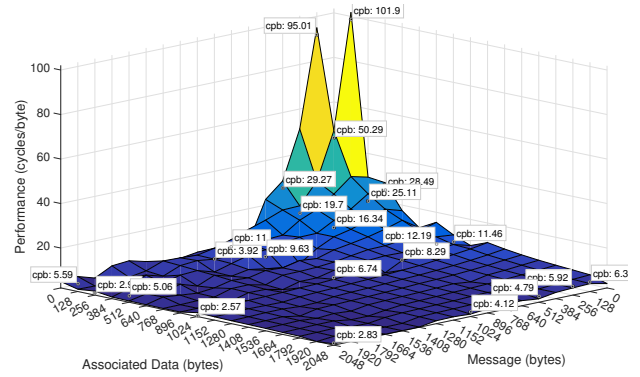


Figure 52: aeadaes256ocbtglen128v1_opt

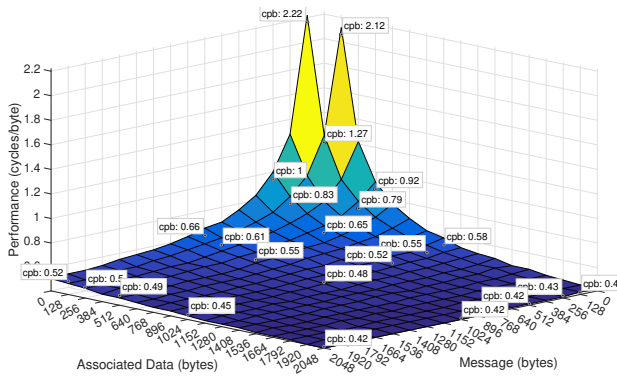


Figure 53: aegis128l_aesnic

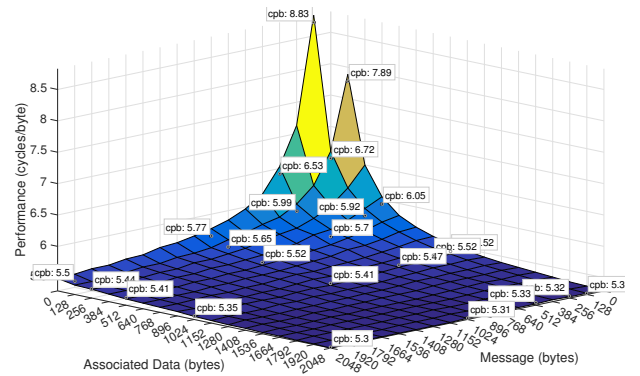


Figure 54: aes128n8t8clocv2_aesni

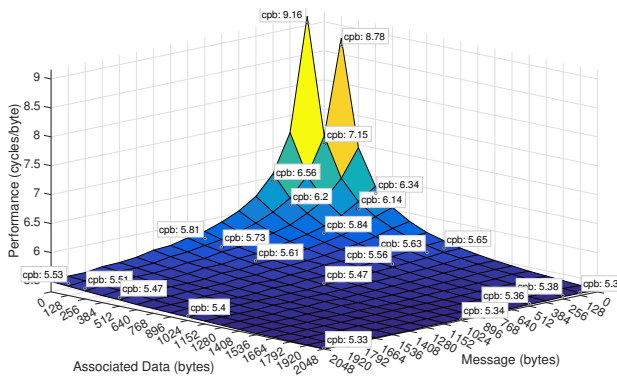


Figure 55: aes128n8t8silcv2_aesni

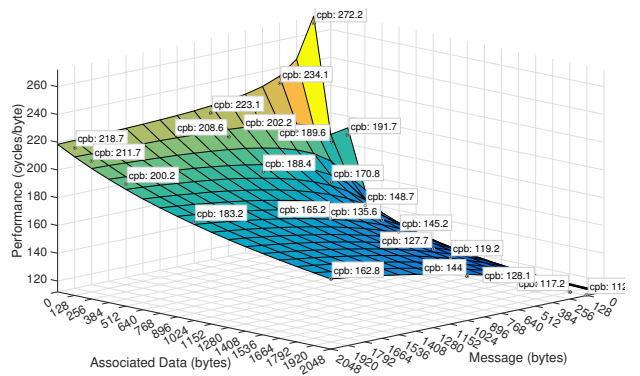


Figure 56: aescopav2_ref

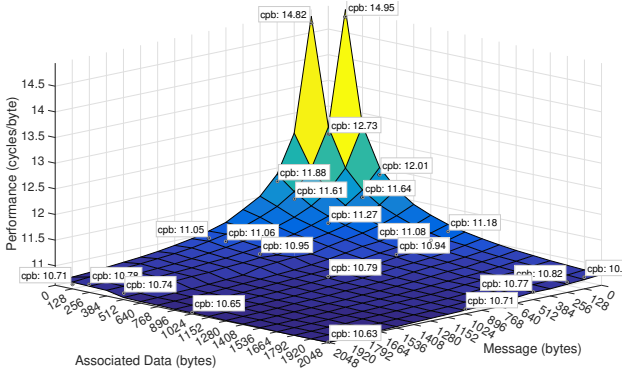


Figure 57: aesjambuv2_aesni

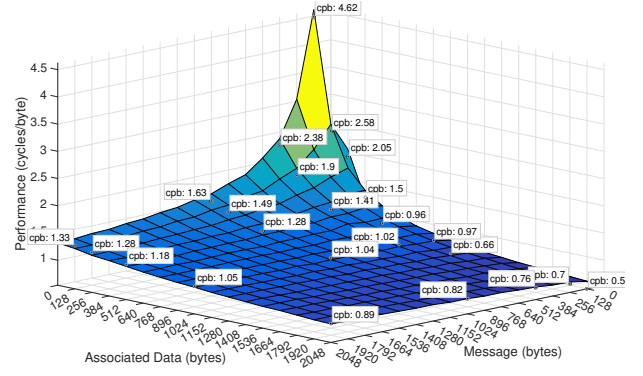


Figure 58: aezv4_aesni

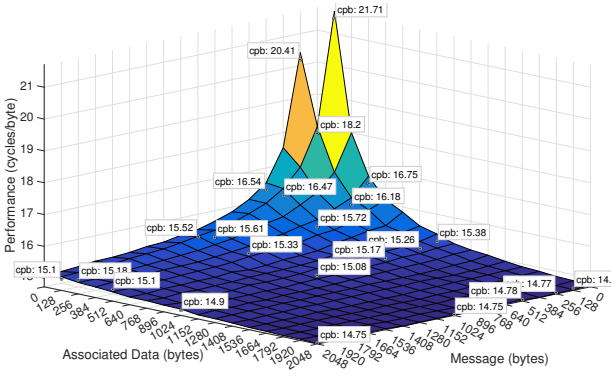


Figure 59: ascon128av11_opt64

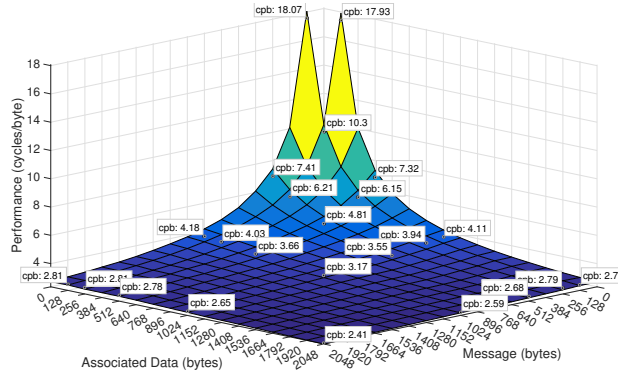


Figure 60: deoxysneq256128v13_aesni

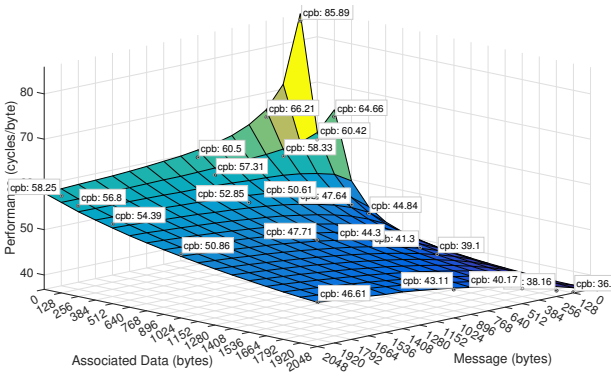


Figure 61: elmd600v2_ref

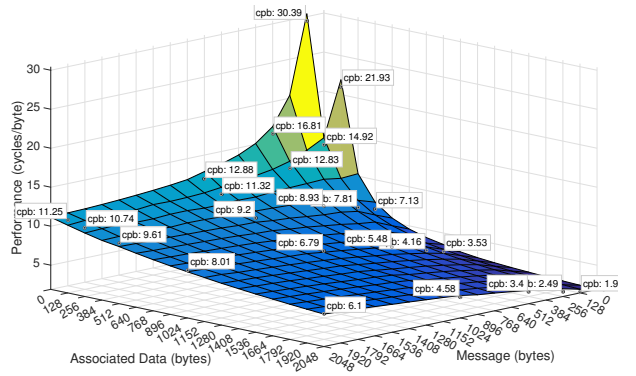


Figure 62: hs1sivlv1_ref

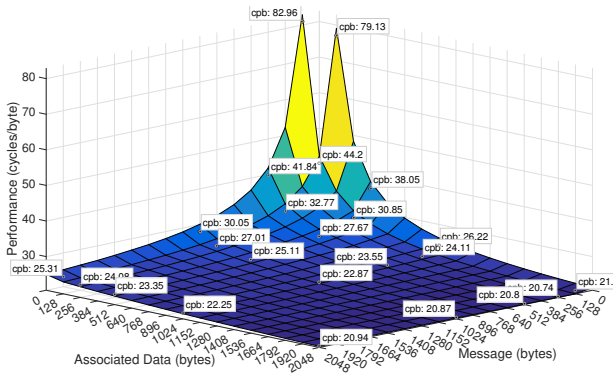


Figure 63: icepole128av2_ref

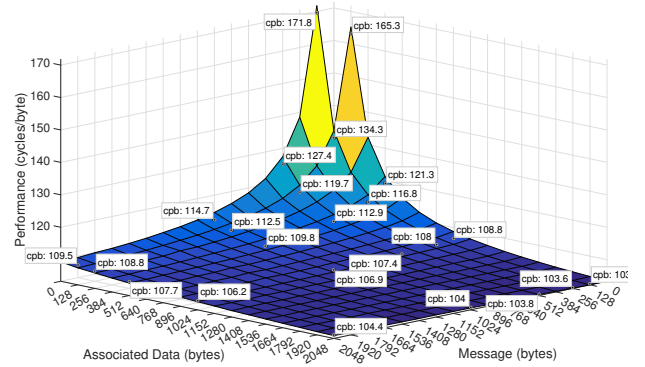


Figure 64: ketjesrv1_reference

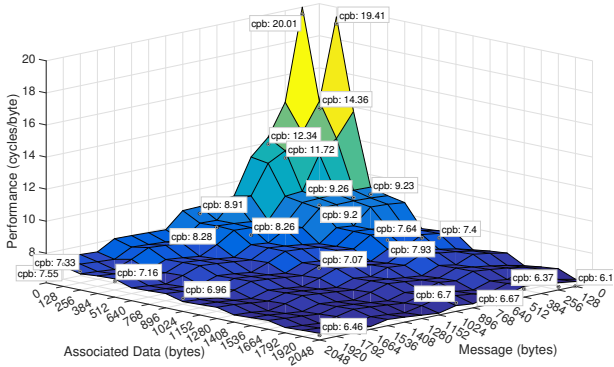


Figure 65: lakekeykv2_generic64lc

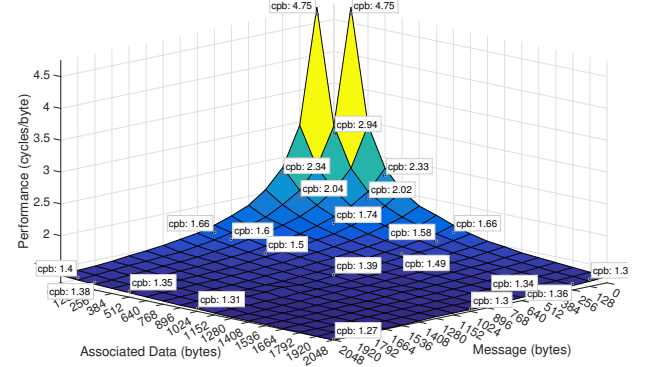


Figure 66: morus640128v1_sse2

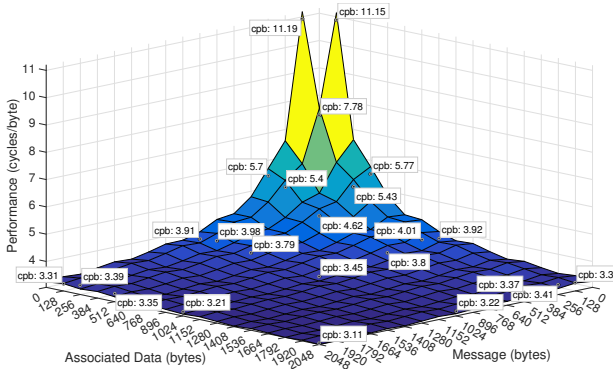


Figure 67: norx6441_xmm

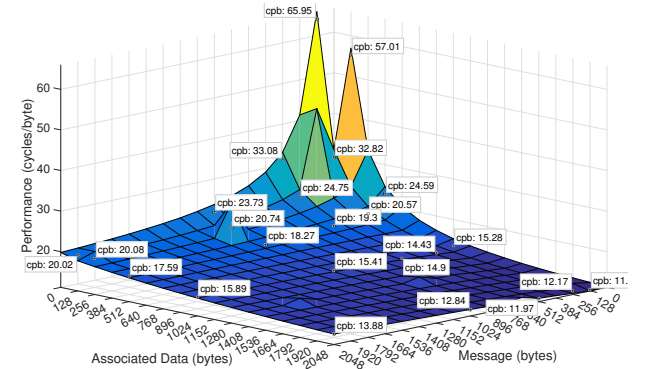


Figure 68: omdsha512k512n256tau256v2_avx1

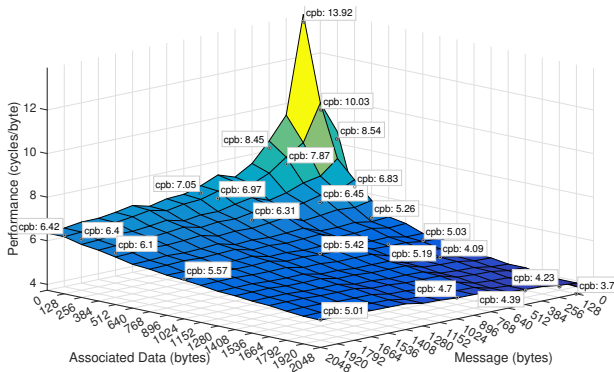


Figure 69: paeq64_aesni

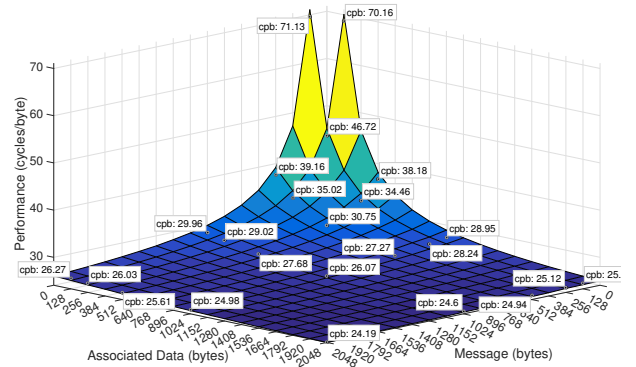


Figure 70: pi64cipher128v2_ref

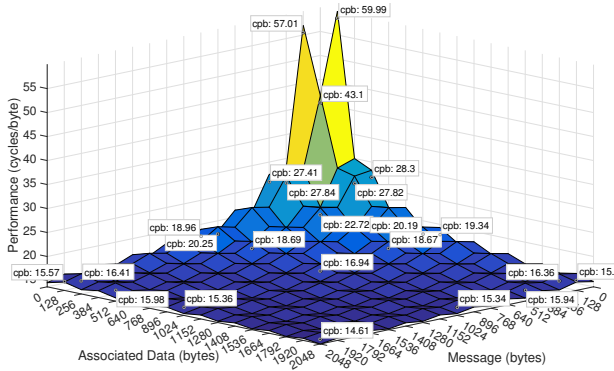


Figure 71: scream10v3_sse

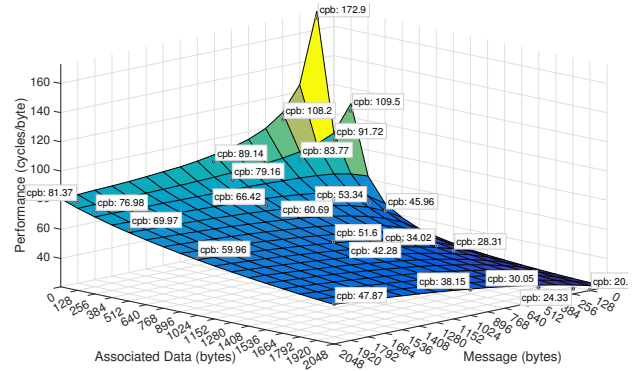


Figure 72: shellaes128v2d4n80_ref

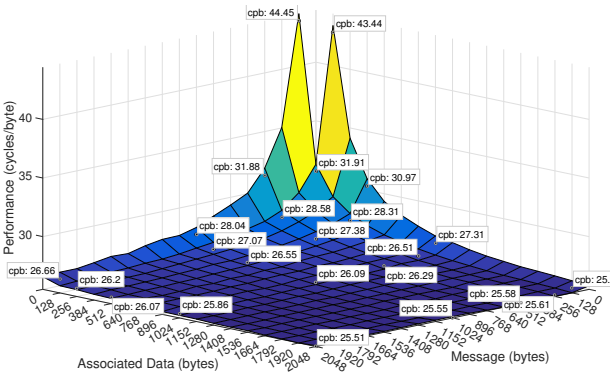


Figure 73: stribob192r2_ssse3

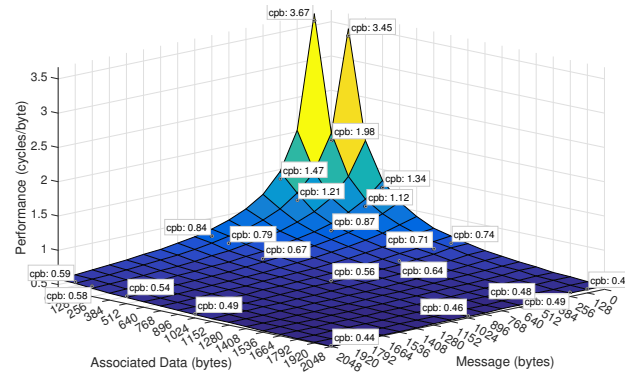


Figure 74: tiaoxin2_nim

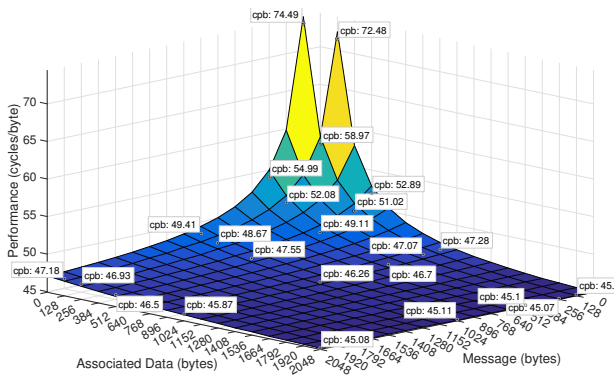


Figure 75: trivia0v2_ref

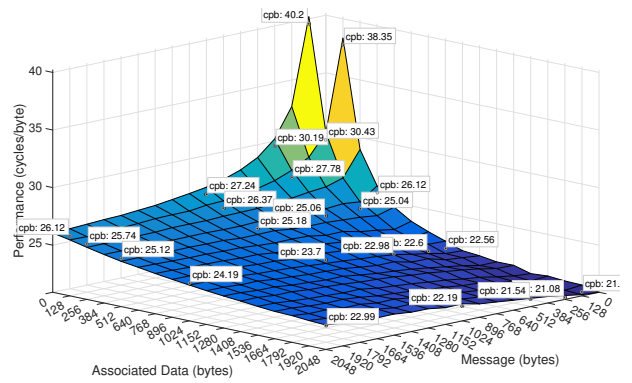


Figure 76: aes128otrsv2_ref

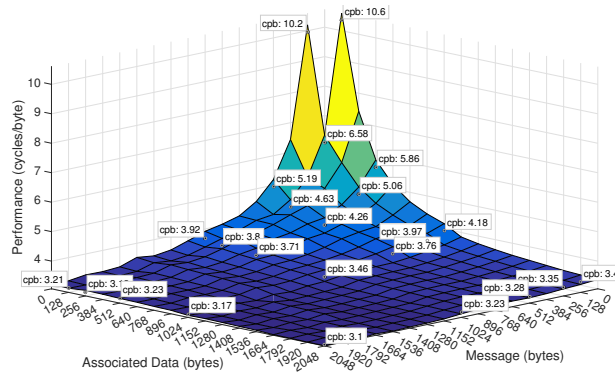


Figure 77: aes128poetv2aes4ls0lt0_ni

D Bar Charts for Real-World Message Sizes for each CAESAR Candidate

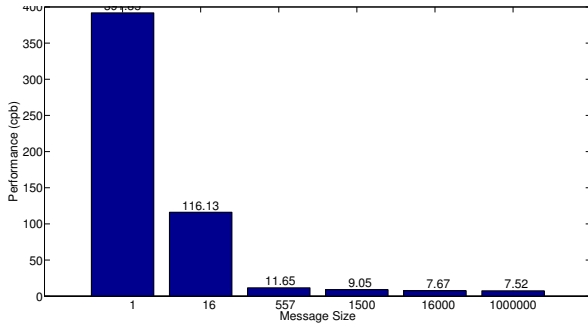


Figure 78: acorn128v2_opt

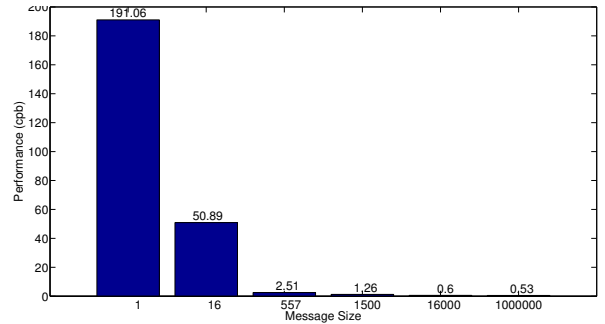


Figure 79: aeadaes128ocbtagn128v1_opt

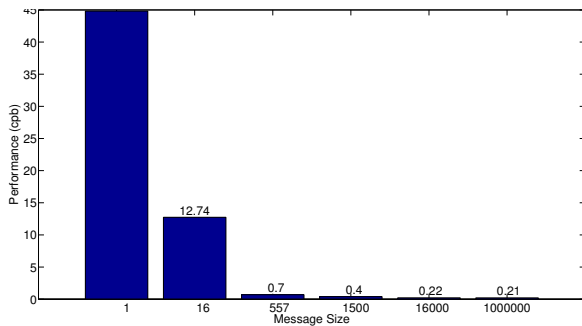


Figure 80: aegis1281_aesnic

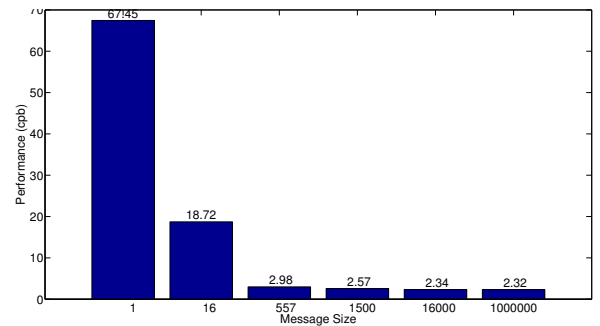


Figure 81: aes128n12t8clocv2_aesni

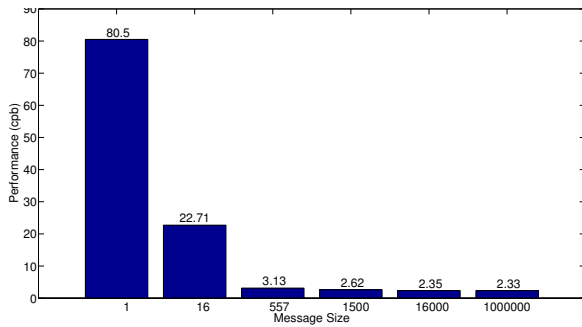


Figure 82: aes128n8t8silcv2_aesni

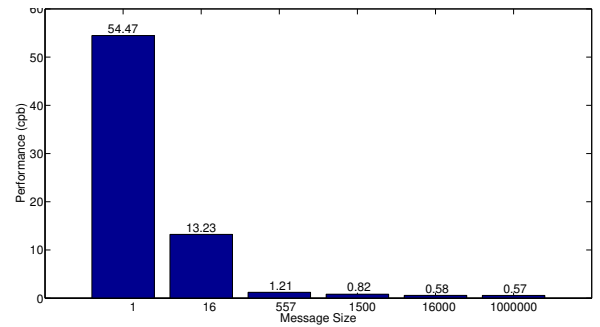


Figure 83: aes128otrpv3_ref

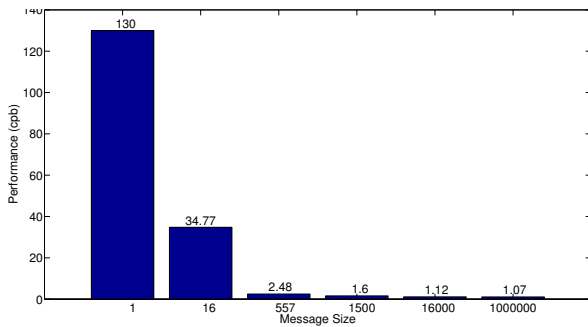


Figure 84: poetv2aes4_ni

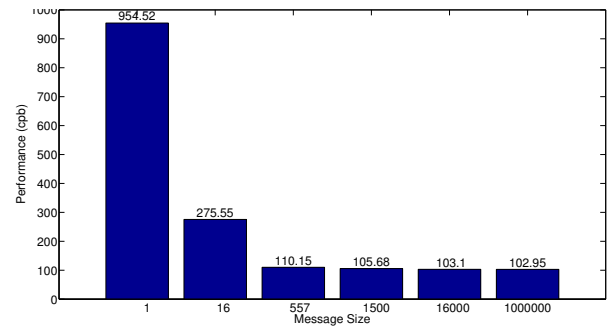


Figure 85: aescopav2_ref

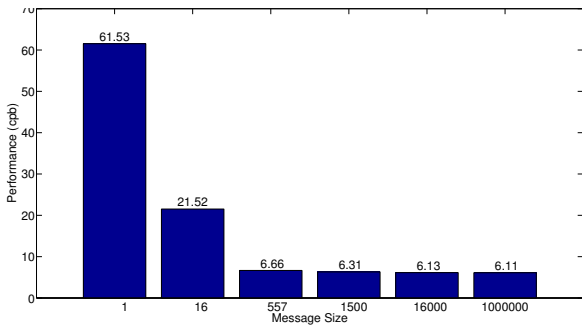


Figure 86: aesjambuv2_aesni

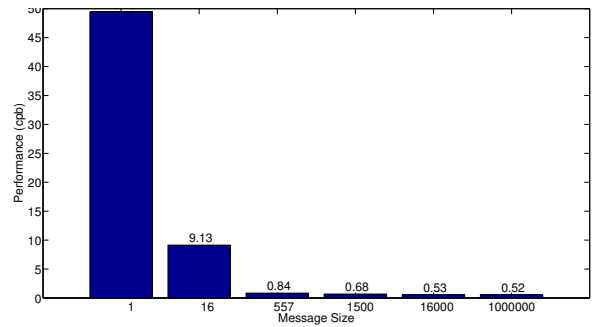


Figure 87: aezv4_aesni

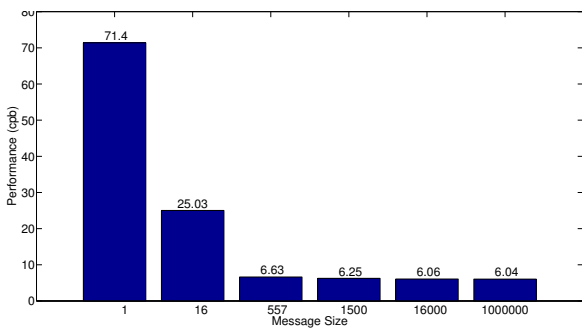


Figure 88: ascon128av11_opt64

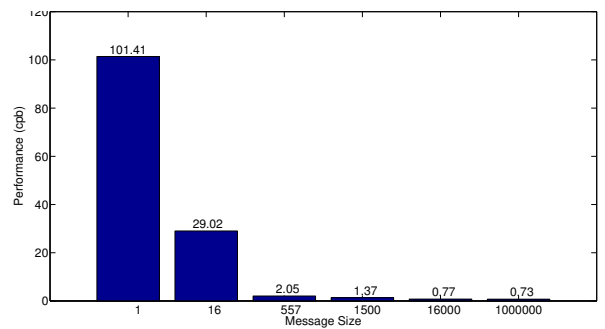


Figure 89: deoxysneq128128v13_aesni

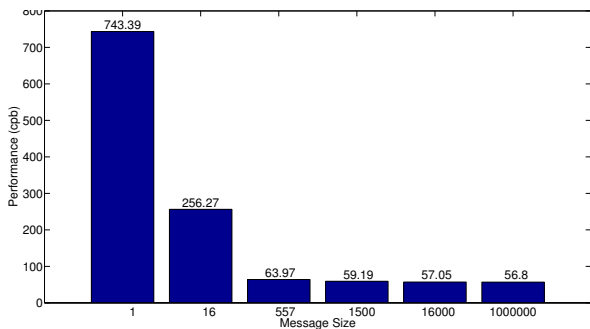


Figure 90: elmd600v2_ref

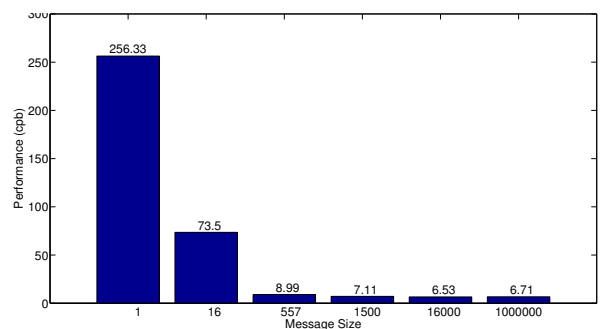


Figure 91: hs1sivlov1_ref

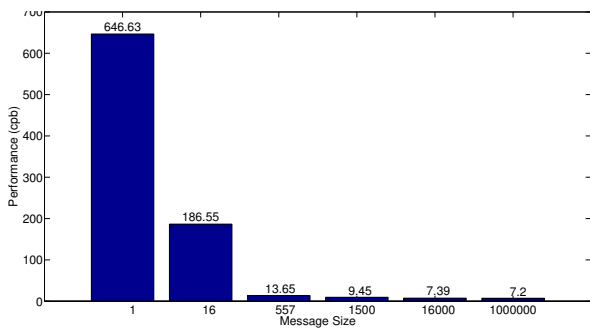


Figure 92: icepole128av2_ref

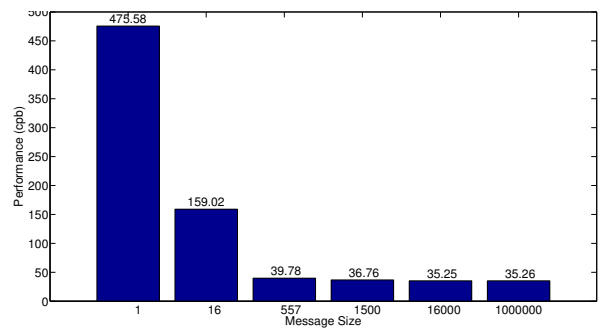


Figure 93: ketjesrv1_reference

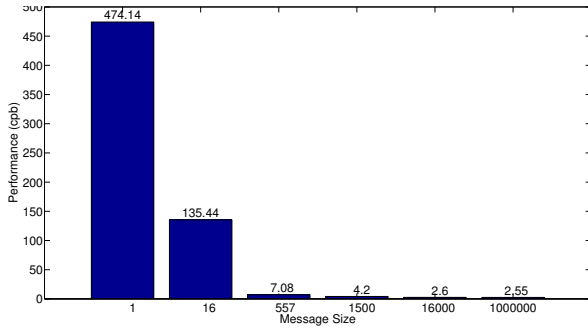


Figure 94: seakeyakv2_SandyBridge

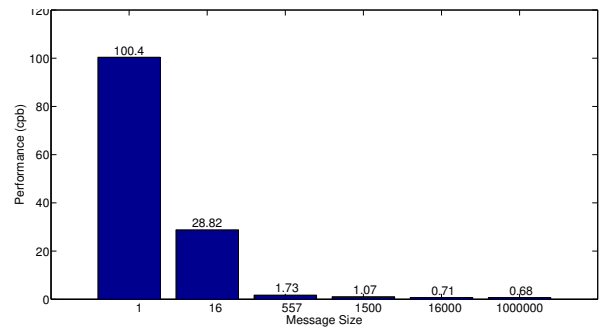


Figure 95: morus1280256v1_avx2

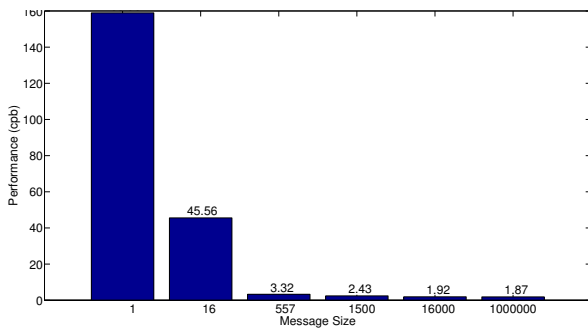


Figure 96: norx6441_ymm

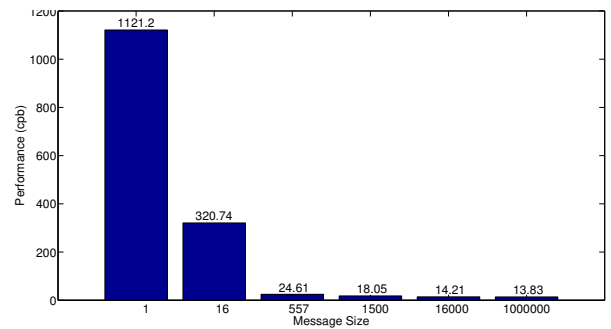


Figure 97: omdsha512k512n256tau256v2_avx1

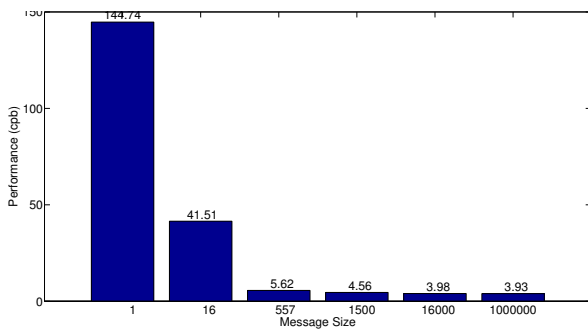


Figure 98: paeq80_aesni

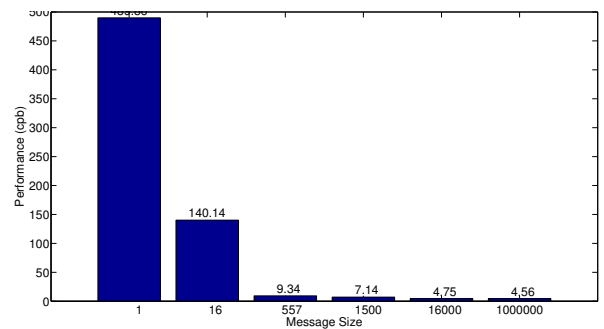


Figure 99: pi64cipher128v2_goptv

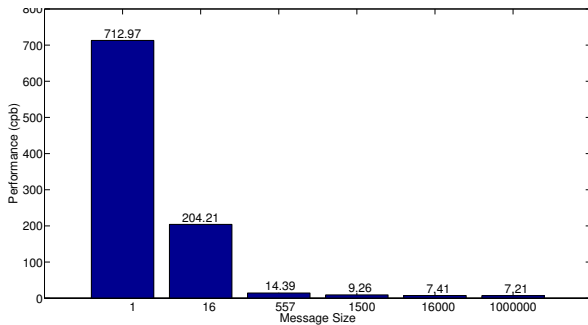


Figure 100: scream10v3_sse

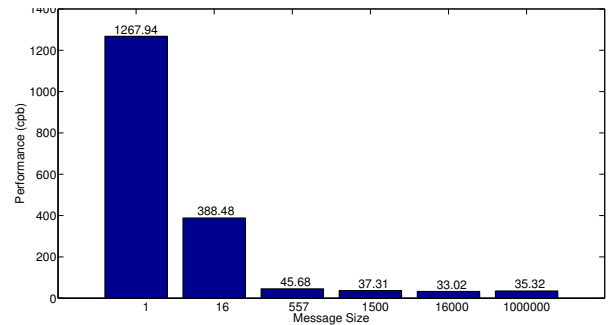


Figure 101: shellaes128v2d8n80_ref

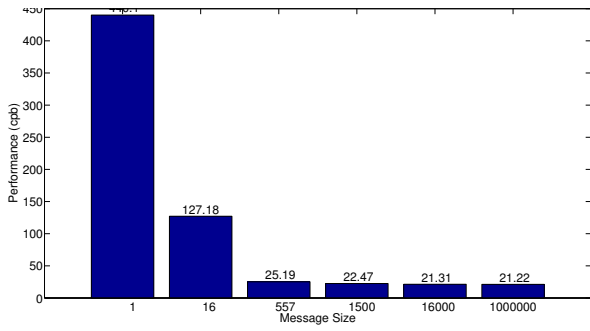


Figure 102: sribob192r2_sse3

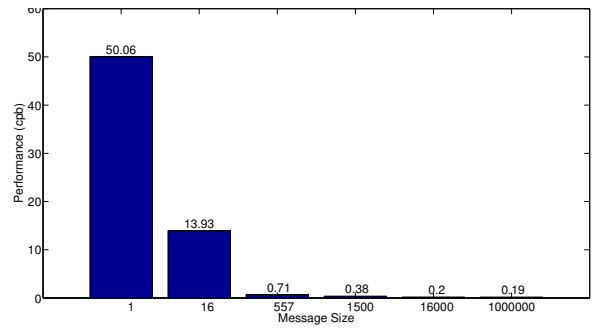


Figure 103: tiaoxinv2_nim

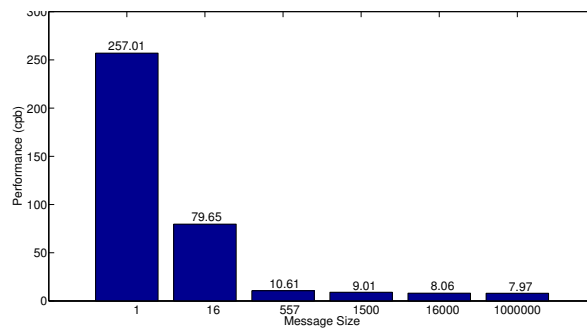


Figure 104: trivia0v2_sse4